JOURNAL OF Materials CHEMISTRY
Feature Article

Manganese oxide porous crystals

Qi Feng,*[a] Hirofumi Kanoh[b] and Kenta Ooi[b]

[a] *Research Laboratory of Hydrothermal Chemistry, Faculty of Science, Kochi University, 2–5-1 Akebono-cho, Kochi-shi, 780–8520, Japan. E-mail: feng@cc.kochi-u.ac.jp*
[b] *Shikoku National Industrial Research Institute, 2217–14 Hayashi-cho, Takamatsu-shi, 761–0395, Japan. E-mail: ooi@sniri.go.jp*

Received 10th July 1998, Accepted 29th October 1998

This article reviews the structure, synthesis, host–guest reaction in aqueous phase, and ion-sieve and molecular-sieve properties of porous manganese oxide crystals. Tunnel and layered manganese oxides constitute a large family of porous materials having pore size from ultramicropores to mesopores. The manganese oxide crystals consist of MnO_6 octahedral units shared by corners and/or edges. They can be prepared by using various metal ions or organic surfactants as templates. The templates are extracted/inserted topotactically from/into the tunnels or interlayer spaces of the manganese oxides by two different mechanisms: redox-type and ion-exchange-type. These manganese oxides show excellent ion-sieve and molecular-sieve properties for the adsorptions of cations or organic molecules. The adsorptive selectivities are dependent on their structures.

Introduction

Porous crystals have potential and are interesting materials due to their specific properties and diversity of structures. Aluminosilicates, including zeolites, clay minerals, and mesoporous silicates, are well known families of porous crystals.[1,2] Recently, much attention has been focused on the porous materials of transition metal oxides.[2,3] Manganese oxides with tunnel and layered crystal structures can constitute a large family of porous materials from ultramicropore to mesopore. Most of the structural frameworks of the manganese oxides consist of MnO_6 octahedral units shared by corners and/or edges,[4] in comparison with, in general, SiO_4(tetrahedral)–AlO_6(octahedral) frameworks of the porous aluminosilicates.

Since these manganese oxides exhibit excellent cation-exchange and molecule adsorptive properties, they can be used as ion-sieves,[5] molecular-sieves,[6] and catalysts[7] similar to the aluminosilicates. Advanced separation and sensing technologies have been developed by application of the ion-sieve properties.[8–11] The excellent electrochemical and magnetic properties of the manganese oxides are also attracting much attention for cathodic materials in lithium batteries[12–19] and new magnetic materials[20–25] during the last decade.

The purpose of this article is to review the structure, synthesis, host–guest reaction in aqueous phase, and the applications of the porous manganese oxide crystals with tunnel and layered structures, mainly during the last decade, and to point out potential new directions in this field. Advances in the fields of the use of manganese oxides with tunnel and layered structures as materials for non-aqueous batteries and in magneto-resistance applications are adequately covered elsewhere in the literature[12–25] and are not included here.

Structures of porous manganese oxide crystals

Many kinds of porous manganese oxide crystals with tunnel and layered structures have been reported. The structural diversity of the manganese oxides is attributed to the characteristics of both ready conversion between Mn^{IV} and Mn^{III} and formation of defects in the crystals, which also account for why it is difficult to get large single crystals for structural studies. Most structural information, therefore, is obtained from powder diffraction, IR spectroscopy, high resolution transmission electron microscopy (HRTEM), and extended X-ray absorption fine structure (EXAFS).

Turner and Buseck[26] have proposed that tunnel and layered manganese oxide minerals can be classified into the pyrolusite-ramsdellite family with $(1\times n)$ tunnel structure, the hollandite-romanechite family with $(2\times n)$ tunnel structure, and the todorokite family with $(3\times n)$ tunnel structure, respectively. The structures all contain infinite chains of edge-shared MnO_6 octahedral structural units, and the numbers 1, 2, 3, and n correspond to the number of octahedra in the unit chain width. The chains are linked by corner sharing to form a one-dimensional tunnel structural network. When $n=\infty$, the network corresponds to a layered structure.

Table 1 shows the major tunnel and layered manganese oxides, according to the nomenclature proposed by Turner and Buseck.[4,26] The schematic structures of several manganese oxides with one-dimensional tunnel and layered structures are shown in Fig. 1. Pyrolusite-, ramsdellite-, hollandite-, romanechite- and todorokite-type manganese oxides,[4,26–29] and synthetic $Rb_{0.27}MnO_2$[30] have one-dimensional (1×1), (1×2), (2×2), (2×3), (3×3), and (2×5) tunnel structures, respectively. On the other hand, birnessite- and buserite-type manganese oxides have layered structures with basal spacings of about 0.7 and 1.0 nm, respectively.[4,27,31,32]

Metal ions can occupy the tunnels of hollandite-, romanechite-, and todorokite-type manganese oxides and $Rb_{0.27}MnO_2$, and also the interlayer spaces of the birnessite- and buserite-type manganese oxides. Crystal water molecules are accommodated also in the tunnels of hollandite-, romanechite-, and todorokite-type manganese oxides, and the interlayer spaces of birnessite- and buserite-type manganese oxides. The birnessite and buserite structures contain a single crystal water sheet and a double crystal water sheet between the MnO_6 octahedral sheets, respectively. Most Mn is tetravalent in these manganese oxides, but a part of the Mn is trivalent to balance the charge of the foreign ions in the tunnels and interlayers.

The intergrowth of two or more tunnel phases occurs also in the manganese oxides. An irregular intergrowth of (1×1) tunnels (pyrolusite) and (1×2) tunnels (ramsdellite) in the structure of γ-MnO_2 (nsutite) is well known to electrochemists [Fig. 2(a)].[4,33,34] Complex intergrowths of the (2×2) tunnels (hollandite) and the (2×3) tunnel (romanechite) in fibrous manganese oxide minerals,[35] as shown in Fig. 2(b), and intergrowth of (3×2) tunnels to (3×7) tunnels in natural todorokite[26] have been detected also by HRTEM measurements. Almost all the intergrowths are random, so that regular periodicity or superstructure may not be apparent.[4]

Table 1 Classification of tunnel and layered manganese oxides and their crystallographic data

Mineral or compound	Approximate formula	Crystal system (space group)	Lattice constants (Å, °)	Structural features
$(1\times n)$ family				
Pyrolusite (β-MnO_2)	MnO_2	Tetragonal ($P4_2/mn2$)	$a=4.39$; $c=2.87$	(1×1) tunnel
Ramsdellite	MnO_2	Orthorhombic ($Pbnm$)	$a=4.53$; $b=9.27$; $c=2.87$	(1×2) tunnel
Nsutite (γ-MnO_2)	$[Mn^{II}, Mn^{III}, Mn^{IV}](O,OH)_2$	Hexagonal	$a=9.65$; $c=4.43$	$(1\times1)/(1\times2)$ complex tunnel
$LiMn_2O_4$		Cubic ($Fd3m$)	$a=8.25$	(1×3) tunnel
$Li_{1.09}Mn_{0.91}O_2$		Hexagonal ($R3m$)	$a=2.85$; $c=14.26$	$(1\times\infty)$ layer 4.75 Å wide
Vernadite (δ-MnO_2)	$MnO_2{\cdot}H_2O{\cdot}R_2O,RO,R_2O_3$ (R = Na,Ca, Co, Fe, Mn)	Hexagonal	$a=2.86$; $c=4.7$	$(1\times\infty)$ layer 4.7 Å wide
$(2\times n)$ family				
Hollandite	$(R)_2[Mn_8]O_{16}{\cdot}xH_2O$ (R = Ba, K, Na, NH_4)	Tetragonal ($I4/m$) or monoclinic ($I2/m$)	$a=9.96$; $c=2.86$ $a=10.03$; $b=5.76$; $c=9.90$; $\beta=90.42$	(2×2) tunnel
Romanechite or psilomelane	$(R)_2[Mn_5]O_{10}{\cdot}xH_2O$ (R = Ba, K, Na)	Monoclinic ($A2/m$)	$a=9.84$; $b=2.88$; $c=13.85$; $\beta=92.30$	(2×3) tunnel
RUB-7	$(R)_2[Mn_6]O_{12}{\cdot}xH_2O$ (R = Rb, K, Na)	Monoclinic ($C2/m$)	$a=14.19$; $b=2.85$; $c=24.34$; $\beta=91.29$	(2×4) tunnel
$Rb_{0.27}MnO_2$	$(Rb)_4[Mn_7]O_{14}$	Monoclinic ($A2/m$)	$a=15.04$; $b=2.89$; $c=14.64$; $\beta=92.4$	(2×5) tunnel
Birnessite	$Na_4Mn_{14}O_{27}{\cdot}9H_2O$ and $R_yMnO_2{\cdot}xH_2O$ (R = monovalent or divalent metal ions)	Orthorhombic Hexagonal, monoclinic, orthorhombic, or triclinic	$a=8.54$; $b=15.39$; $c=14.26$	$(2\times\infty)$ layer about 7 Å wide
$(3\times n)$ family				
Todorokite	$(R)[Mn_6]O_{18}{\cdot}xH_2O$ (R = divalent metal ions and Na, K)	Monoclinic ($P2/m$)	$a=9.76$; $b=2.84$; $c=9.55$; $\beta=94.1$	(3×3) tunnel
Buserite	$Na_yMnO_2{\cdot}xH_2O$ and $R_yMnO_2{\cdot}xH_2O$ (R = divalent metal ions)	Hexagonal	$a=8.41$; $c=10.01$	$(3\times\infty)$ layer about 10 Å wide
Lithiophorite	$[Mn^{III}_2Mn^{IV}_4O_{12}][Li_2Al_4(OH)_{12}]$	Monoclinic ($C2/m$)	$a=5.06$; $b=8.70$; $c=9.61$; $\beta=100.7$	Sandwich layer about 9.5 Å apart
Other families				
$Na_{0.44}MnO_2$		Orthorhombic ($Pbam$)	$a=9.10$; $b=26.34$; $c=2.82$	MnO_6/MnO_5 complex tunnel
$Li_{0.44}MnO_2$		Orthorhombic ($Pbam$)	$a=8.93$; $b=24.44$; $c=2.83$	MnO_6/MnO_5 complex tunnel
$Ba_6Mn_{24}O_{48}$		Tetragonal ($I4/m$)	$a=18.17$; $c=2.824$	$(1\times1)\times(2\times2)$ complex tunnel
α-$NaMnO_2$		Monoclinic ($C2/m$)	$a=5.63$; $b=2.86$; $c=5.77$; $\beta=112.9$	Layer 5.3 Å wide
α-$LiMnO_2$		Monoclinic ($C2/m$)	$a=5.44$; $b=2.81$; $c=5.39$; $\beta=116.0$	Layer 4.8 Å wide
β-$NaMnO_2$		Orthorhombic ($Pmnm$)	$a=2.85$; $b=6.31$; $c=4.77$	Layer 6.31 Å wide
β-$LiMnO_2$		Orthorhombic ($Pmnm$)	$a=2.81$; $b=5.75$; $c=4.57$	Layer 5.75 Å wide
MOMS-1	Mn_2O_3/Mn_3O_4	Hexagonal	$a=54$; $c=\infty$	Mesopore size about 30 Å
MOMS-2	Mn_2O_3/Mn_3O_4	Cubic ($Ia3d$)		Mesopore

In addition to the one-dimensional $(m\times n)$ tunnel families, other types of tunnel and layered structures have been also reported. The spinel structure shows a three-dimensional (1×3) network tunnel by connecting 8a tetrahedral sites and empty 16c octahedral sites of a cubic closed-packed oxygen framework (Fig. 3).[36] A series of the spinel-type lithium manganese oxides which can be expressed by the general formula $Li_nMn_{2-x}O_4$ ($1\leqslant n\leqslant1.33$, $0\leqslant x\leqslant0.33$, $n\leqslant1+x$) can be formed.[37–39] (Li)$[Mn^{III}Mn^{IV}]O_4$ and (Li)$[Li_{0.33}Mn^{IV}{}_{1.67}]O_4$ are two typical spinel-type lithium manganese oxides, where () and [] are 8a tetrahedral sites and 16d octahedral sites, respectively, of a cubic closed-packed oxygen framework of the spinel structure. In (Li)$[Mn^{III}Mn^{IV}]O_4$ spinel, Li^+ occupy the 8a tetrahedral sites and Mn^{III} and Mn^{IV} occupy the 16d octahedral sites. In (Li)$[Li_{0.33}Mn^{IV}{}_{1.67}]O_4$ spinel, Li^+ occupy the 8a tetrahedral sites and vacant 16d octahedral sites of manganese, and all the manganese ions are tetravalent.

$Na_{0.44}MnO_2$ has a complex one-dimensional tunnel structure.[40] This tunnel structure is made up by linking MnO_6 octahedral chains and MnO_5 square pyramidal chains, as shown in Fig. 4. There are two types of one-dimensional tunnels in the structure. One is made up by four MnO_6 octahedral units and two MnO_5 square pyramid units; the other by ten MnO_6 octahedral units and two MnO_5 square pyramid units. Na^+ ions are located in both types of tunnels, and they can be substituted with Li^+ to obtain $Li_{0.44}MnO_2$ with a similar structure.[19]

Two types of layered $NaMnO_2$ have been reported. One is α-$NaMnO_2$, having flat edge-shared MnO_6 octahedral sheets similar to birnessite with Na^+ ions between the sheets,[18,40] as

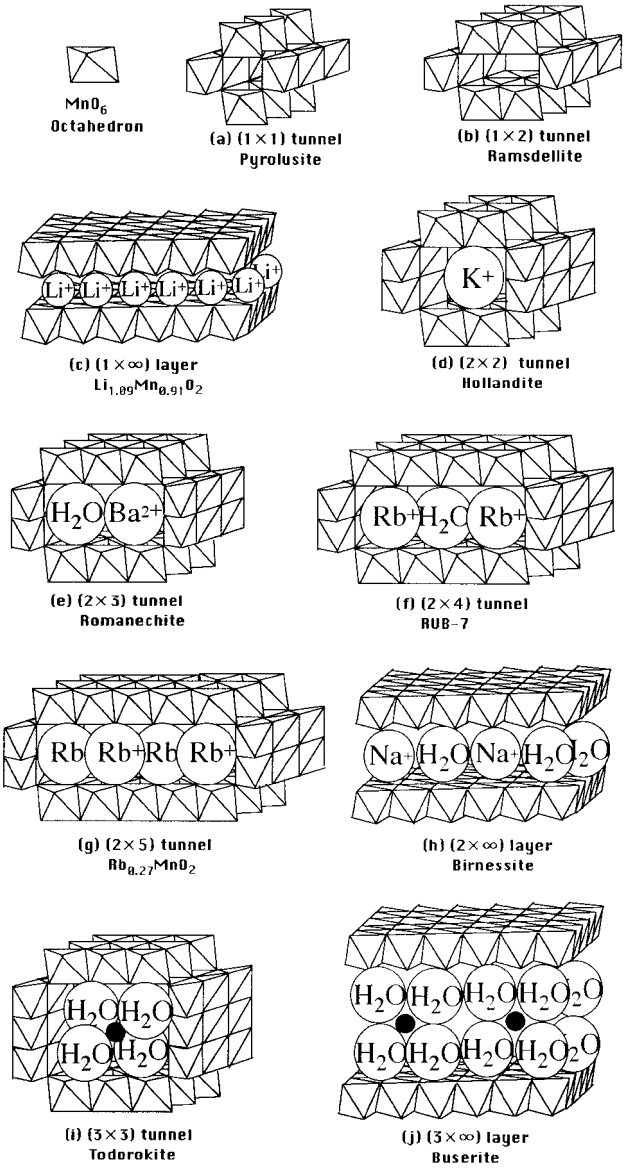

Fig. 1 Schematic structures of one-dimensional tunnel and layered manganese oxides.

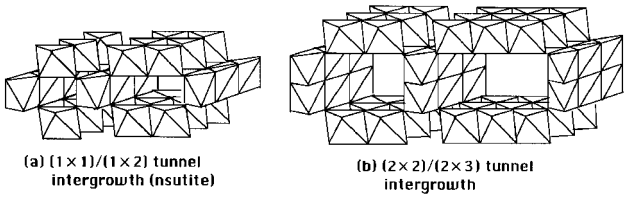

Fig. 2 Intergrowth tunnels of (a) (1×1) and (1×2), and (b) (2×2) and (2×3) in the tunnel manganese oxides.

shown in Fig. 5(a). The other is β-$NaMnO_2$ with zigzag MnO_6 octahedral sheets and Na^+ between the sheets [Fig. 5(b)].[40,41] Two types of $LiMnO_2$ analogous to $NaMnO_2$, where Na^+ are substituted by Li^+, have been also reported.[18,41]

Recently, several new members of the manganese oxide families and new families have been reported. Rossouw *et al.*[42] have reported a new type of $Li_{1.09}Mn_{0.91}O_2$ with a rock-salt layered structure [Fig. 1(c)]. This layered manganese oxide has a MnO_6 octahedral layer similar to α-$LiMnO_2$, but a different Li^+ arrangement. This layered oxide which has a basal spacing of 0.475 nm may be designated $(1\times\infty)$. Rziha *et al.*[43] have reported a new type of Rb-MnO_2 (RUB-7) belonging to a new member of the $(2\times n)$ family. Single crystal

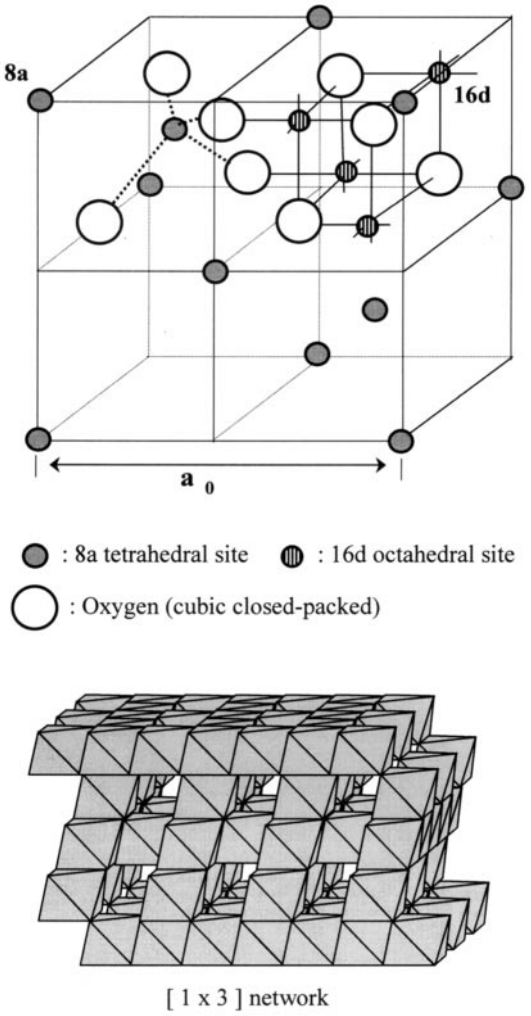

Fig. 3 Structure of spinel-type lithium manganese oxide and its three-dimensional (1×3) tunnel connecting 8a and 16c sites.

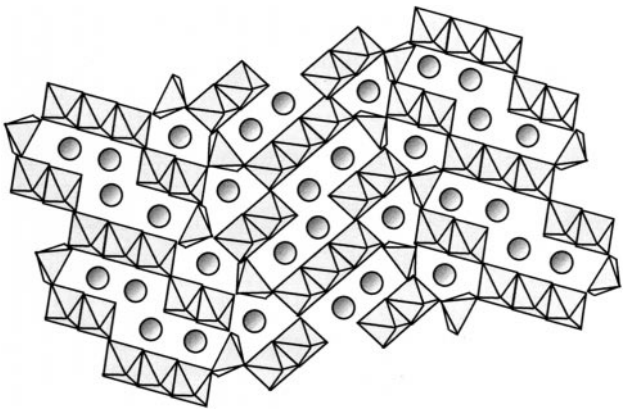

Fig. 4 One-dimensional tunnel structure of $Na_{0.44}MnO_2$ looking down the *c* axis.

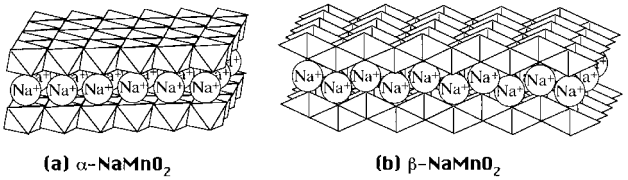

Fig. 5 Schematic structures of (a) α-$NaMnO_2$ and (b) β-$NaMnO_2$.

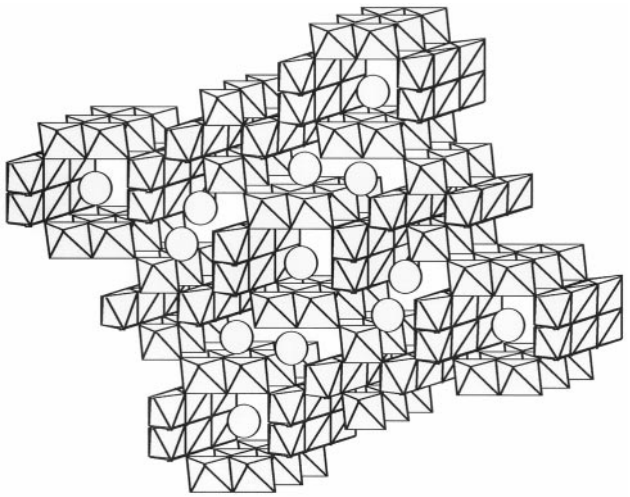

Fig. 6 Structure of $Ba_6Mn_{24}O_{48}$ with complex one-dimensional tunnels.

X-ray diffraction and Rietveld analyses suggest that RUB-7 has a one-dimensional (2×4) tunnel [Fig. 1(f)]. In the tunnel structure, two Rb^+ and one water of crystallisation may occupy a unit tunnel.

Another new type of tunnel manganese oxide is $Ba_6Mn_{24}O_{48}$ with an ordered intergrowth of complex tunnel structure, as shown in Fig. 6.[44] High-resolution electron microscopy and electron diffraction studies show that this structure consists of hollandite (2×2) tunnel and pyrolusite (1×1) tunnel units sharing the edges of their MnO_6 octahedra. In this structure, in addition to the one-dimensional (2×2) and (1×1) tunnels, a new one-dimensional tunnel of ten-MnO_6 units is generated. Ba^{2+} locate at the (2×2) tunnel and ten-MnO_6 tunnel.

Tian *et al.*[45] have reported mesoporous manganese oxides with uniform pore size (Fig. 7). Both hexagonal and cubic phases (MOMS-1 and MOMS-2) which are structurally similar to MCM-41 and MCM-48 silicate materials[46] have been prepared. The mesopore wall materials are made up by microcrystallites of Mn_2O_3 and Mn_3O_4, which are different from most other mesoporous materials, such as silicate type materials, where the walls are composed of amorphous materials.

Synthesis of tunnel and layered manganese oxides

The synthesis of manganese oxide ion-sieves and molecular sieves can be separated into two steps, as schematically represented in Fig. 8. In the first step, a tunnel or layered manganese oxide is prepared by using template ions or molecules to direct its tunnel or layer dimension. In the second step, the templates are removed topotactically from the tunnel or interlayer space to obtain an ion sieve or molecular sieve. In this section we review the preparations of tunnel and layered manganese oxides with various templates.

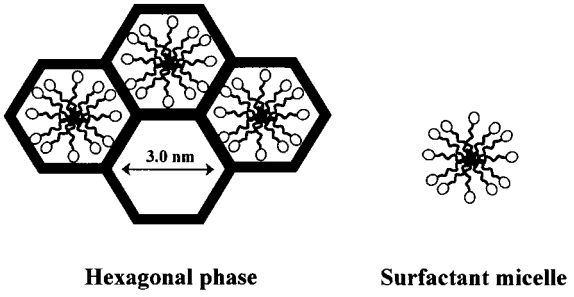

Fig. 7 Schematic representation of hexagonal mesoporous manganese oxide (MOMS-1) and the surfactant micelle template.

The tunnel and layered manganese oxides can be prepared by a variety of processes. These processes can be classified into dry processes (solid state reaction and melting salt flux processes), wet processes (redox precipitation, hydrothermal, and hydrothermal soft chemical processes), and wet–dry processes (sol–gel processes). Stable phases with small tunnel and narrow layered structures, such as spinel, hollandite, romanechite, and birnessite can be prepared by any of these processes. Metastable phases with large tunnel and wide layered structures, such as $Rb_{0.27}MnO_2$, RUB-7, todorokite, buserite, and mesoporous manganese oxides, are prepared only by the wet processes. Metal ions and organic surfactants are usually used as templates (Table 2). The wide tunnel and layered structures are easily formed under high template concentrations. The ion-sieve, electrochemical, and catalytic properties of the manganese oxides are frequently dependent on the synthetic process.

Solid state reaction

In the solid state reaction, metal ions are used as the templates, and the resulting tunnel size and layer width are dependent on the size and quantity of the templates. Manganese compounds ($MnCO_3$, MnO_2, Mn_2O_3, MnOOH, $Mn(CH_3COO)_2$, *etc.*) can be used as manganese sources, and alkali metal compounds (M_2CO_3, MOH, MNO_3, MCH_3COO, *etc.*, here M = alkali metals) as template sources.

Spinel-type manganese oxides are prepared with a Li^+ template. A large number of studies on the synthesis of spinel-type lithium manganese oxides have been carried out, since they are very important as a cathode material for rechargeable batteries.[12] A series of the oxides $Li_nMn_{2-x}O_4$ ($1\leqslant n\leqslant1.33$, $0\leqslant x\leqslant0.33$, $n\leqslant1+x$) can be obtained in a temperature range from 350 to 900 °C.[12,38,47–50] The oxidation number of manganese and composition of the manganese oxides are dependent on the reaction conditions, such as reaction temperature, starting materials, and reaction atmosphere. $(Li)[Mn^{III}Mn^{IV}]O_4$ spinel is easily formed under high temperature conditions (> 700 °C), and $(Li)[Li_{0.33}Mn^{IV}_{1.67}]O_4$ spinel under low temperature conditions (< 500 °C).

Ooi *et al.*[51] have investigated the template effect of alkali metal ions in the solid reaction process. The authors calcined γ-MnO_2 into which metal ions (Li^+, Na^+ or K^+) had been introduced at 600 °C for 2 h. A spinel was obtained with a Li^+ template, and hollandites with Na^+ and K^+ templates.

A systematic study on the synthesis of sodium manganese was carried out by Parant *et al.*[40] A series of the tunnel and layered sodium manganese oxides ($Na_{0.20}MnO_2$, $Na_{0.40}MnO_2$, $Na_{0.44}MnO_2$, $Na_{0.70}MnO_2$, α-$NaMnO_2$ and β-$NaMnO_2$) can be formed in this solid state reaction system. $Na_{0.20}MnO_2$, $Na_{0.40}MnO_2$, $Na_{0.44}MnO_2$, and $Na_{0.70}MnO_2$ have hollandite, romanechite, complex tunnel, and birnessite analogous layered structures, respectively. In the layered $NaMnO_2$ system, α-$NaMnO_2$ and β-$NaMnO_2$ are formed in low and high temperature ranges, respectively.

Using Na^+ as a template for the hollandite and romanechite is rare, because the size of Na^+ is somewhat smaller than the tunnel sizes of hollandite or romanechite types. In the solid state reaction, K^+ is usually used as a template for the hollandites.[52]

Melting salt flux process

It is difficult to obtain large crystalline samples of porous manganese oxides. However, the melting salt flux process can grow some single crystals of microporous manganese oxides. Recently, Boullay *et al.*[44] have prepared a new type of tunnel manganese oxide ($Ba_6Mn_{24}O_{48}$) by using the melting salt flux process. The needle-shaped single crystals of the new type of tunnel manganese oxide were prepared by reacting $BaCO_3$ and MnO_2 in a Bi_2O_3 melting salt at 1270 °C. $BaMnO_3$ was also

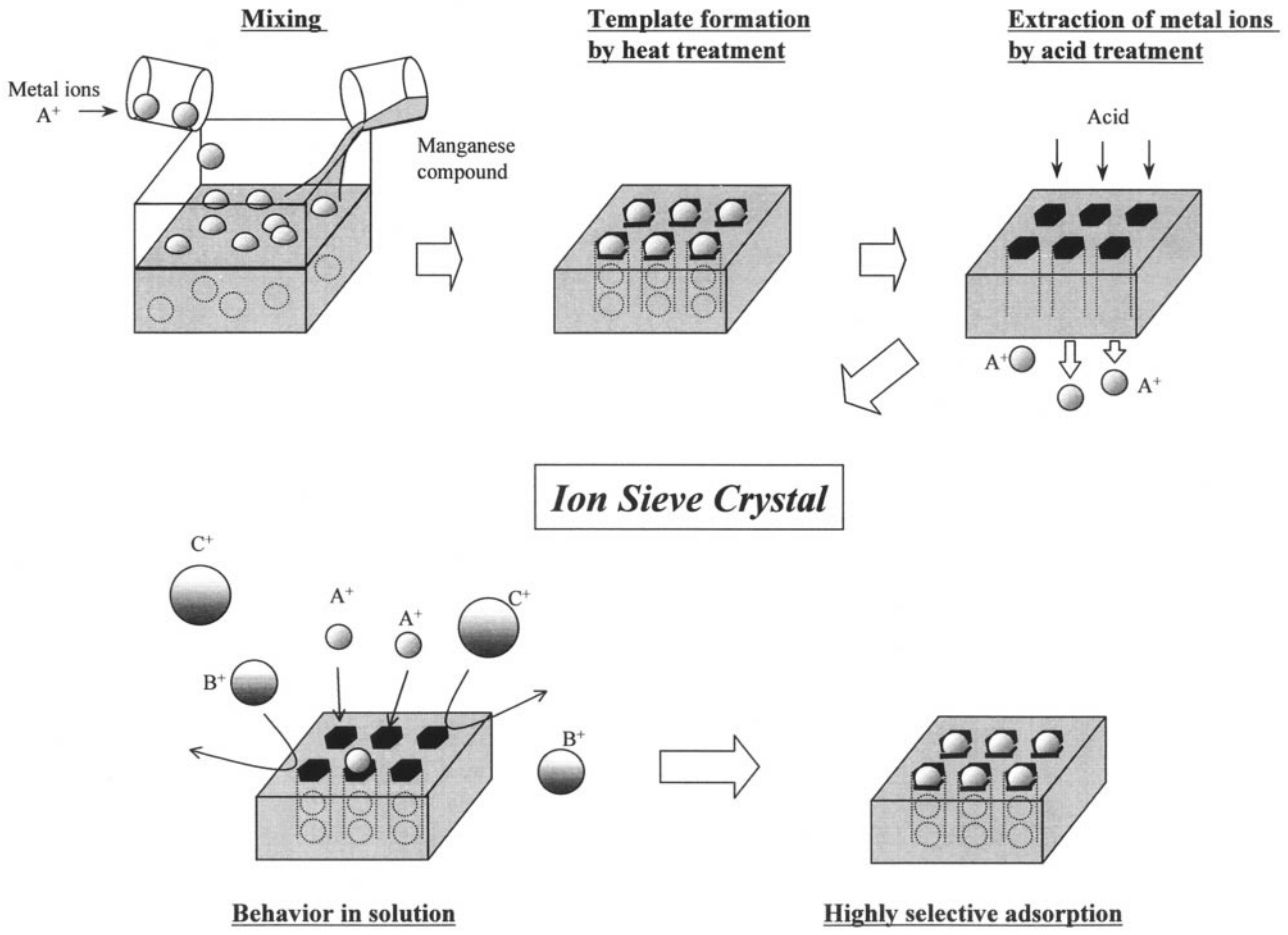

Fig. 8 Schematic representation of synthesis of manganese oxide ion-sieve and ion-sieve behavior.

Table 2 Synthesis of tunnel and layered manganese oxides with various templates

	Template	
Compound	Wet process	Dry or wet–dry process
Pyrolusite (β-MnO_2)	H^+	No template
Ramsdellite	H^+	
Spinel	Li^+	Li^+, Mg^{2+}
$A_{0.44}MnO_2$		Na^+
α-$AMnO_2$		Na^+
β-$AMnO_2$		Li^+, Na^+
Hollandite	K^+, Rb^+, Ba^{2+}, NH_4^+, H_3O^+	K^+, Ba^{2+}, Na^+
Romanechite	Ba^{2+}	Na^+
RUB-7	Rb^+, K^+, Na^+	
$Rb_{0.27}MnO_2$	Rb^+	
Birnessite	Alkali metal ions	Na^+, K^+
$Ba_6Mn_{24}O_{48}$		Ba^{2+}
Buserite	Na^+	
Todorokite	Mg^{2+}, divalent transition metal ions	
MOMS	$CH_3(CH_2)_{15}(CH_3)_3N^+$, $[CH_3(CH_2)_3]_4N^+$	

formed as an impurity in the product. In this reaction, Ba^{2+} acts as the template for the (2×2) and ten-MnO_6 tunnels. Also, Tang *et al.* have prepared well crystallized orthorhombic $LiMnO_2$ using a (LiCl + LiOH) flux.[53]

Redox precipitation process

The precipitation process involving oxidation of Mn^{II} salts and/or reduction of MnO_4^- salts in solutions is a typical method for the production of synthetic manganese oxides. Birnessite and hollandite are frequently prepared by using this process. Birnessite can be obtained in alkaline or weak acidic solution, while the hollandite can be obtained only in acidic solution.

The Giovanoli method[54,55] or its modifications are well known for the preparation of birnessite. The process is divided into two steps. In the first step, NaOH solution is added into MnX_2 ($X^- = Cl^-$, NO_3^-, *etc.*) solution to produce a $Mn(OH)_2$ precipitate, and in the second step, the precipitate is bubbled with oxygen or air in the solution while cooling with vigorous stirring to oxidize Mn^{II} [$Mn(OH)_2$] to Mn^{IV} and Mn^{III} (birnessite). The oxidation accompanies insertions of Na^+ and H_2O into the interlayer of the birnessite structure. Other oxidants, *e.g.* Cl_2 and MnO_4^-, can also be used in this process.[16,32,56] The M-birnessites (M = Li, K, Rb, or Cs) are produced in MOH solutions instead of Na-birnessite in NaOH solution.[16,32,57,58]

Feng *et al.* have developed a convenient process for the preparation of birnessite-type manganese oxides.[59–62] In this process, a mixed solution of NaOH and H_2O_2 is added quickly into a MnX_2 solution while rapidly stirring at room temperature. The precipitation of $Mn(OH)_2$ and the oxidation to birnessite are achieved immediately. Birnessite containing another cation (Li^+, K^+, Rb^+, or Cs^+) can be obtained by using a different alkaline solution instead of NaOH.

The hollandite-type manganese oxides can be prepared directly by oxidation of Mn^{II} salts or reduction of $AMnO_4$ in acidic aqueous solution. K^+ and NH_4^+ are usually used as the template for the preparation of hollandites. K-hollandites are prepared by reacting $MnSO_4$ or $Mn(NO_3)_2$ solution with $KMnO_4$ or $KClO_3$ in a 1 M H_2SO_4 solution at above 60 °C.[63–65] NH_4-hollandites are obtained by using $NH_4S_2O_8$ as the oxidant.[66,67]

The hollandites without template metal ions in the tunnel sites can be directly prepared by reacting $Mn(NO_3)_2$ with $LiMnO_4$ or $NaMnO_4$,[14] or oxidation of $MnSO_4$ with ozone (O_3) gas in a H_2SO_4 solution.[68] In these reactions, H_3O^+ may act as the template for the hollandite structure. A higher reaction temperature (>70 °C) and higher concentration of H_2SO_4 (>4 M) are necessary for the hollandite formation than when using a K^+ or NH_4^+ template.

Mesoporous manganese oxides have been prepared by using the redox precipitation process with surfactant micelle template. Hexagonal and cubic phases can be obtained by partial oxidation of $Mn(OH)_2$ with air in cetyltrimethylammonium bromide (CTAB) solution.[45] The partial oxidation reaction accompanies incorporation of surfactant micelles with $Mn(OH)_2$. The resulting products are dependent on the concentration of CTAB. The hexagonal phase is formed in a 28% solution, and cubic phase in a 10% solution. The template micelles can be removed by calcination in air. Another mesoporous manganese oxide has been prepared by reduction of $(C_{12}H_{25})NMe_3MnO_4$ with ethanol in $(C_{12}H_{25})NMe_3OH$ solution.[69]

Sol–gel process

For the preparation of a low-temperature spinel phase of high purity, some sol–gel processes have been developed. Barboux *et al.* have prepared $Li_xMn_2O_4$ spinel by precipitating $Mn(CH_3COO)_2$ solution with LiOH and calcining the precipitate at 300 °C.[70] Takada *et al.*[71,72] have prepared a well crystallized $Li_4Mn_5O_{12}$ spinel by heating a eutectic mixture of LiOAc and $Mn(NO_3)_2$ at 700 °C in an O_2 atmosphere. Bach *et al.*[73,74] have developed a sol–gel process for spinel and birnessite. $AMnO_4$ [A = Li, Na, K, NH_4, $N(CH_3)_4$] were reduced by fumaric acid ($C_4H_4O_4$) at room temperature to form an amorphous xerogel. Spinel phase and $LiMnO_2$ are prepared by heat treatment of the $LiMnO_4$–$C_4H_4O_4$ gel at 600 and 1000 °C, respectively. Layered manganese oxides [Na-birnessite (600 °C), α-$NaMnO_2$ (800 °C), β-$NaMnO_2$ (1100 °C), and $KMnO_2$ (600 °C)] can be obtained by heat treatment of $NaMnO_4$–$C_4H_4O_4$ or $KMnO_4$–$C_4H_4O_4$ gels. However, NH_4^+ and $N(CH_3)_4^+$ ions cannot act as templates for tunnel and layered manganese oxides, due to their instability at high temperature.

Ching *et al.* have reported the sol–gel synthesis of birnessite and hollandite with polyols as reductant.[75,76] A xerogel is obtained by reacting $NaMnO_4$ or $KMnO_4$ solution with glucose solution with rapid stirring. The xerogel is washed with water to remove Na^+ or K^+ adsorbed on the particle surface. Birnessite and hollandite can be obtained by calcining the $KMnO_4$–glucose gel. Birnessite is formed at high K/Mn ratio, and hollandite under low K/Mn ratio conditions. In the $NaMnO_4$–glucose reaction system, a birnessite but not hollandite is obtained, due to the fact that Na^+ is not a suitable template for the hollandite structure.

Hydrothermal process

Many types of tunnel and layered manganese oxides can be produced using a hydrothermal process. Studies on the synthesis of spinel, birnessite, hollandite, and (2 × 5) tunnel phases have been reported. Spinel and birnessite can be prepared by hydrothermally treating γ-MnO_2 in LiOH and NaOH or KOH solutions, respectively.[77,78] The birnessites are also obtained by hydrothermally treating β-MnO_2 or α-Mn_2O_3 in a NaOH solution.[79,80]

Endo *et al.*[81] have reported that hollandite and birnessite are formed by hydrothermal decomposition of $KMnO_4$. The hollandite is formed at both higher temperature and lower pressure than the conditions for birnessite formation. A $K_2Mn_4O_9$ phase is obtained in this hydrothermal decomposition reaction.

For the development of new type lithium battery materials, preparation of hollandites by treatment of manganese oxides in hot acid solution have been studied. Ohzuku *et al.*[82] have prepared hollandites with NH_4^+, K^+, and Rb^+ templates by treating Mn_2O_3 in 0.5 M H_2SO_4 solutions containing these ions at 100 °C. The hollandite without the template ions in the tunnel can be obtained by leaching Mn_2O_3 in a 4–8 M H_2SO_4 solution at 105 °C.[83] The treatment of Mn_2O_3 in acidic solution results in the disproportionation of Mn_2O_3 into soluble Mn^{2+} and MnO_2 with a hollandite structure. Rossouw *et al.*[84] have synthesized a highly crystalline hollandite without metal ion or NH_4^+ in the tunnel by leaching Li_2MnO_3 in a 1–4 M H_2SO_4 solution at 90 °C. Similar to the redox precipitation reaction, the H_3O^+ ions may act as the template in these reactions.

Yamamoto *et al.*[30,85] have prepared a $Rb_{0.27}MnO_2$ with (2 × 5) tunnel structure by hydrothermally reacting β-MnO_2 in 5 M RbOH at >400 °C. Four Rb^+ act as the template for one unit tunnel size in the formation reaction of the (2 × 5) tunnel. Hollandite and birnessite phases are also formed in the hydrothermal reaction system. The structure of the manganese oxide is strongly dependent on the concentration of RbOH.[86] The product is hollandite at conditions of low RbOH concentration, while the product is (2 × 5) manganese oxide or birnessite-type manganese oxide at high RbOH concentration. This suggests that large tunnel and layered structures are preferred in alkaline solution at high template concentrations.

Hydrothermal soft chemical process

A hydrothermal soft chemical process[87] is a useful and unique method for the preparation of the tunnel manganese oxides. This process comprises two steps: the first step is the preparation of a framework precursor with layered or analogous structure and insertion of template ions or molecules into the interlayer space by a soft chemical reaction, and the second step is the transformation of the template-inserted precursor into a tunnel or other structure by hydrothermal treatment. The dimension of the resulting tunnel can be designed and predicted easily from the dimensions of the template.

A typical soft chemical process uses birnessite or buserite as precursor. About 50 years ago, Wadsley[88] reported that a Ba^{2+}-exchanged birnessite can be transformed to a romanechite under hydrothermal conditions. Later, Golden *et al.*[89,90] found a todorokite can be formed by hydrothermal treatment of a Mg^{2+}-exchanged birnessite at 155 °C. The early studies, however, were carried out from a geological standpoint to understand the formation processes of manganese oxide minerals in nature.

Recently this method has been used for the synthesis of manganese oxide ion-sieves and molecular-sieves. Shen *et al.*[6] prepared a thermally stable (up to 500 °C) todorokite by doping Mg^{2+} on Mn^{IV} sites for the development of octahedral molecular-sieves. For development of manganese oxide ion-sieves, Feng *et al.*[87,91] have carried out systematic studies on the effect of template on tunnel size under low temperature hydrothermal conditions. Spinel, hollandite, romanechite, and todorokite phases can be obtained by using Li^+, K^+, $Ba(H_2O)_2^{2+}$, and $Mg(H_2O)_4^{2+}$ templates, respectively (Fig. 9). A good crystalline birnessite is obtained by using a Na^+ template.[60] When H^+ acts as the template in acidic solutions, pyrolusite and ramsdellite are formed. The sizes of the resulting tunnels correspond to the sizes of the templates.

Recently, Rziha *et al.*[43] have reported that a new type of tunnel manganese oxide (RUB-7) with one-dimensional (2 × 4) tunnel structure can be formed by hydrothermally treating a M-birnessite (M = Rb, K, Na) in MOH at 350 °C. Luo *et al.*[69] have reported that organic cations can also be used as a template in the transformation reaction of birnessite to tunnel manganese oxide. A mesoporous manganese oxide is obtained by using tetrabutylammonium template ions.

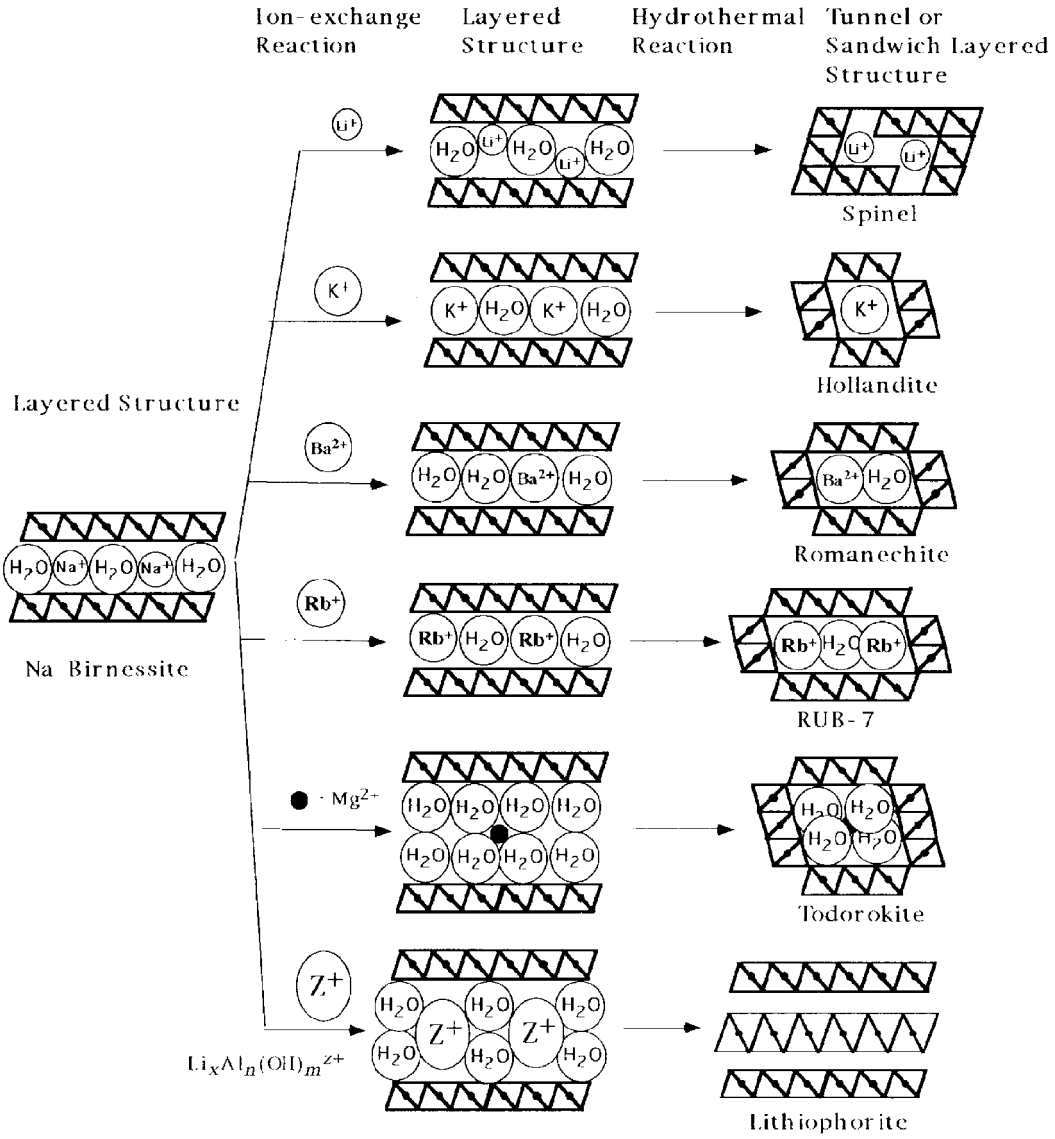

Fig. 9 Transformation reactions from birnessite to tunnel and sandwich layered manganese oxides under hydrothermal conditions.

When using $Li_xAl_n(OH)_m^{z+}$ hydroxide complex ions as a template,[92] lithiophorite with a sandwich layered structure, as shown in Fig. 10, is obtained, instead of a tunnel manganese oxide. The formation of the sandwich layered structure can be described as follows. The $Li_xAl_n(OH)_m^{z+}$ complex ions in the interlayer space hydrolyze and polymerize together to form large complex ions under hydrothermal conditions (Fig. 9). Since the layered structure of birnessite acts as a template in the polymerization reaction, the polymerization occurs two dimensionally, and forms the $LiAl_2(OH)_6$ octahedral cation sheet between the MnO_6 octahedral sheets of the birnessite structure.

Several methods can be used also for the transformation of the layered structure to the tunnel structure; for example,

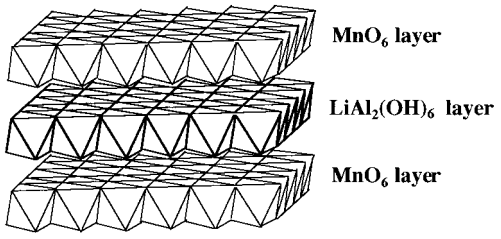

Fig. 10 Sandwich layered structure of lithiophorite.

hollandite can be obtained by calcining K-, Ba- or Na-birnessite.[93–95] The hydrothermal reaction, however, may be most effective for the transformation reaction, because under hydrothermal conditions the transformation reaction can be carried out at low temperature to prevent destruction of metastable tunnel structures, and the template ion or molecule can be incorporated/liberated into/from the precursor from/to the solution phase to reach a composition for the desired structure during the transformation reaction.[91]

Extraction/insertion reactions with metal ions

To obtain manganese oxide ion-sieves, the template ions in the tunnels and interlayer spaces must be removed by a topotactic extraction reaction with acid. After the extraction treatment, metal ions can enter into the tunnels and the interlayer spaces again by topotactic reaction. There are two types of reactions in the extraction and insertion of metal ions. One is an ion-exchange-type reaction, and the other a redox-type reaction.

Spinel-type manganese oxide

Vol'khin *et al.*[96,97] first found that a spinel-type manganese oxide without metal ions in the tunnel can be obtained by extracting Li^+ from a spinel-type lithium manganese with an

acid. The spinel-type manganese oxide shows Li^+ adsorptive properties. Hunter[98] has proposed a redox mechanism for the Li^+ extraction reaction from $(Li)[Mn^{III}Mn^{IV}]O_4$ spinel:

$$4(Li)[Mn^{III}Mn^{IV}]O_4 + 8H^+ \rightarrow$$
$$3(\ )[Mn^{IV}{}_2]O_4 + 4Li^+ + 2Mn^{2+} + 4H_2O \quad (1)$$

The driving force for the extraction reaction is a disproportionation reaction of Mn^{III} to Mn^{IV} and Mn^{II} under acidic conditions. The redox-type extraction of one Li^+ is attended by the disproportionation of one Mn^{III} by the reaction $Mn^{III} \rightarrow 1/2Mn^{IV} + 1/2Mn^{II}$, and all Mn are tetravalent in the Li^+-extracted spinel. The manganese oxide has empty 8a tetrahedral sites, and is designated as λ-MnO_2. Li^+ can re-enter the empty sites in the Li^+-extracted spinels. Ooi *et al.*[99,100] have proposed a redox mechanism:

$$(\ )[Mn^{IV}{}_2]O_4 + LiOH \rightarrow$$
$$(Li)[Mn^{III}Mn^{IV}]O_4 + 0.5H_2O + 0.25O_2 \quad (2)$$

for the insertion. In this reaction, Mn^{IV} are reduced to Mn^{III} with O_2 gas evolution to maintain the electroneutrality of the spinel.

On the other hand, Shen *et al.*[101] have studied a spinel-type lithium manganese oxide, and suggested the Li^+ extraction/insertion reaction is an ion-exchange reaction. Studies[38,49,50,102] on the Li^+ extraction/insertion reactions for a series of spinel-type lithium manganese oxides have indicated that the redox-type and ion-exchange-type reactions are dependent on the oxidation number of Mn and distribution of metal ions in the spinel. The Li^+ extraction/insertion reactions of the $(Li)[Li_{0.33}Mn^{IV}{}_{1.67}]O_4$ spinel progress by an ion-exchange mechanism:

$$(Li)[Li_{0.33}Mn^{IV}{}_{1.67}]O_4 + 1.33H^+ \rightleftarrows$$
$$(H)[H_{0.33}Mn^{IV}{}_{1.67}]O_4 + 1.33Li^+ \quad (3)$$

In this spinel, since all Mn are tetravalent, the disproportionation reaction of Mn^{III} does not occur under acidic conditions.

The Li^+ extraction/insertion sites in the spinel-type manganese oxides can be classified as redox-type $\{(Li)[Mn^{III}Mn^{IV}]O_4\}$ and ion-exchange-type $\{(Li)[Li_{0.33}Mn^{IV}{}_{1.67}]O_4\}$.[38] One Mn^{III} ion in the spinel corresponds to the formation of one redox-type site, and one Mn defect in the 16d octahedral site to the formation of four ion-exchange sites. In most real spinel-type manganese oxides, the redox-type sites and ion-exchange sites are intermixed, sharing the Mn–O framework of the spinel, to form a one-phase solid solution system. In such cases, the extraction/insertion reactions of Li^+ can be written schematically as in Fig. 11. The dissolution of Mn^{2+} according to the redox reaction (1) proceeds at the surface of the powder owing to the free movement of electrons. The dissolution may proceed for the Mn atoms on the surface regardless of whether it comprises a redox site or an ion-exchange site.

Sato *et al.*[103] have studied Li^+ extraction/insertion reactions for the spinel-type lithium manganese oxides prepared by different methods, and indicated that the redox reaction and ion-exchange reaction are dependent on the preparation conditions of the spinel-type manganese oxides. The Li^+–H^+ ion exchange reaction is possible at the surface of the $(Li)[Mn^{III}Mn^{IV}]O_4$ spinel.

A series of spinel-type manganese oxides can be obtained by doping the spinel-type lithium manganese oxide with divalent and trivalent metal ions.[37] These spinel-type manganese oxides can be classified as redox-type and ion-exchange-type on the basis of our model (Table 3). The redox-type spinels contain metal ions which can be oxidized to a higher valence when Li^+ are extracted from the spinels. For example, Mn^{III} and Co^{II} can be oxidized to Mn^{IV} and Co^{III}

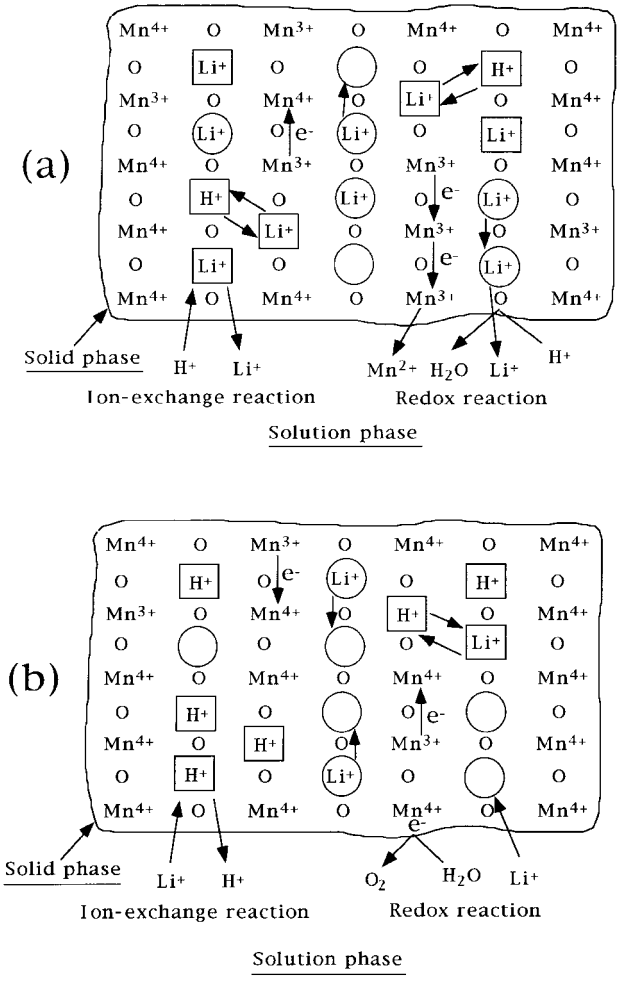

Fig. 11 Schematic representation of (a) Li^+ extraction reaction and (b) Li^+ insertion reactions with spinel-type manganese oxide ion-sieve in one-phase solid solution system. ○: redox-type site, □: ion-exchange-type site.

Table 3 Classification of spinel-type manganese oxides

Redox-type spinel	Ion-exchange-type spinel
$(Li)[Mn^{III}Mn^{IV}]O_4$	$(Li)[Li_{0.33}Mn^{IV}{}_{1.67}]O_4$
$(Li)[Mn^{III}Ti^{IV}]O_4$	$(Li)[Mg^{II}{}_{0.5}Mn^{IV}{}_{1.5}]O_4$
$(Li)[Co^{II}{}_{0.5}Mn^{IV}{}_{1.5}]O_4$	$(Li_{0.5}Zn^{II}{}_{0.5})[Li_{0.5}Mn^{IV}{}_{1.5}]O_4$
$(Mg)[Mn^{III}{}_2]O_4$	$(Li)[Al^{III}Mn^{IV}]O_4$
	$(Li_{0.6}Fe^{III}{}_{0.4})[Li_{0.4}Fe^{III}{}_{0.6}Mn^{IV}]O_4$
	$(Li)[Co^{III}Mn^{IV}]O_4$
	$(Mg)[MgMn^{IV}]O_4$

during the Li^+ extraction reactions, respectively. On the other hand, all metal ions are inert towards oxidation in the ion-exchange-type spinels.

The Li^+ extractabilities for the spinel-type manganese oxides are dependent on the metal ion distributions in the spinel structure (Fig. 12).[104–106] The spinels with divalent and trivalent metal ions at the 8a tetrahedral sites $\{(Li_{0.5}Zn^{II}{}_{0.5})[Li_{0.5}Mn^{IV}{}_{1.5}]O_4$ and $(Li_{0.6}Fe^{III}{}_{0.4})[Li_{0.4}Fe^{III}{}_{0.6}Mn^{IV}]O_4\}$ show a lower Li^+ extractability, and larger dependence on preparation temperature than those with Li^+ alone at the tetrahedral sites $\{(Li)[Mn^{III}Mn^{IV}]O_4$, $(Li)[Mg^{II}{}_{0.5}Mn^{IV}{}_{1.5}]O_4\}$. These differences are explained by the metal ion arrangement in the spinel structure.[105] The migration of Li^+ from the bulk crystal to the surface is through 8a→16c→8a→16c pathways, as shown in Fig. 13. When the 8a tetrahedral sites are occupied by immobile or lower mobility metal cations, such as divalent or trivalent

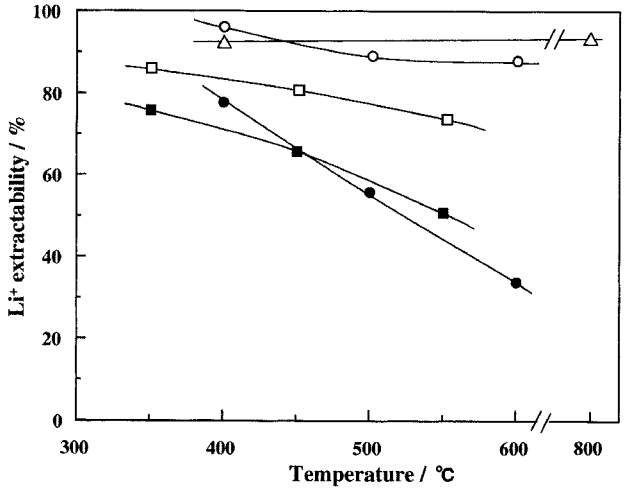

Fig. 12 Effect of preparation temperature on Li^+ extractabilities by acid treatment (1 M HNO_3) for various kinds of spinel-type manganese oxides with different ion distributions in the spinel structure. ●: $(Li_{0.5}Zn^{II}_{0.5})[Li_{0.5}Mn^{IV}_{1.5}]O_4$; ○: $(Li)[Mg^{II}_{0.5}Mn^{IV}_{1.5}]O_4$; ■: $(Li_{0.6}Fe^{III}_{0.4})[Li_{0.4}Fe^{III}_{0.6}Mn^{IV}]O_4$; □: $(Li)[Al^{III}Mn^{IV}]O_4$; △: $(Li)[Li_xMn_{2-y}]O_4$. Reprinted with permission from reference 105. Copyright 1995 American Chemical Society.

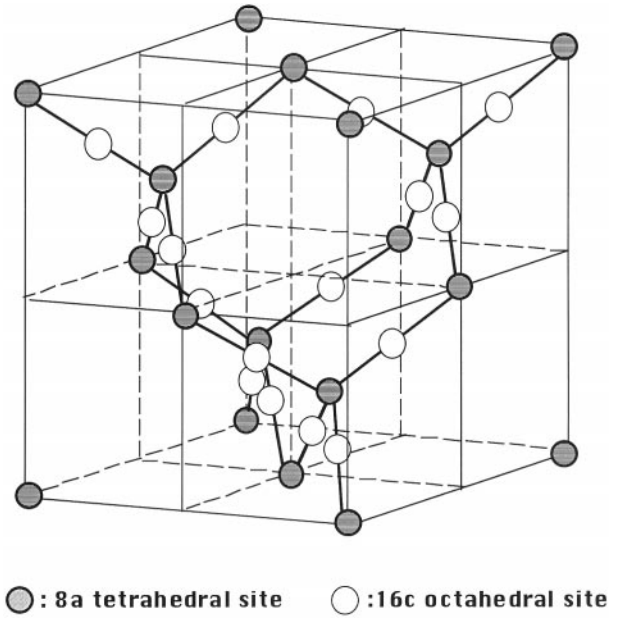

Fig. 13 View of the migration pathway for Li^+ ions in the spinel structure.

metal cations, the Li^+ migration is inhibited by these cations. The remarkable decrease of Li^+ extractability with an increase in preparation temperature for the spinels with divalent or trivalent metal ions at the 8a tetrahedral sites is mainly due to the tendency toward an ordered arrangement of Li^+ and divalent or trivalent metal ions at 8a sites.

Hollandite-type manganese oxide

Tsuji *et al.*[11,63,107] have reported that K^+ in K-hollandite can be extracted by treatment with 13 M HNO_3. All alkali metal ions can enter the lattice of K^+-removed hollandite. The K^+ extraction and metal ion adsorption reactions are topotactic, preserving the hollandite structure. Feng *et al.*[108] have proposed that hollandite-type manganese oxides can be expressed by a general formula $\{A_n\}[\square_x Mn_{8-x}]O_{16}$ ($n \leqslant 2$, $x \leqslant 1$), where {}, [], □, and A denote the (2×2) tunnel sites, octahedral sites for Mn, octahedral vacant sites, and metal ions in the tunnel, respectively. The hollandite-type manganese oxides can be classified also as redox-type and ion-exchange-type similar to the spinel-type manganese oxides. $\{K_2\}[Mn^{III}_2Mn^{IV}_6]O_{16}$ is a redox-type hollandite, and $\{K_2\}[\square_{0.5}Mn^{IV}_{7.5}]O_{16}$ is an ion-exchange-type hollandite. The redox and ion-exchange extraction/insertion reactions for hollandite-type potassium manganese oxides can be written as follows:[108,109]

$$8\{K_2\}[Mn^{III}_2Mn^{IV}_6]O_{16} + 32H^+ \rightarrow$$
$$7\{\ \}[Mn^{IV}_8]O_{16} + 16K^+ + 8Mn^{2+} + 16H_2O \quad (4)$$
$$\{\ \}[Mn^{IV}_8]O_{16} + 2KOH \rightarrow$$
$$\{K_2\}[Mn^{III}_2Mn^{IV}_6]O_{16} + H_2O + (1/2)O_2 \quad (5)$$

for the redox reactions;

$$\{K_2\}[\square_{0.5}Mn^{IV}_{7.5}]O_{16} + 2H^+ \rightleftarrows$$
$$\{H_2\}[\square_{0.5}Mn^{IV}_{7.5}]O_{16} + 2K^+ \quad (6)$$

for the ion-exchange reactions. The redox-type extraction of one K^+ is attended by the disproportionation of one Mn^{III} to $0.5Mn^{II}$ and $0.5Mn^{IV}$. The number of ion-exchange-type sites is four times the number of manganese defects at the octahedral site, similar to the spinel system.

Todorokite-type manganese oxide

Feng *et al.*[59] have studied the metal ion extraction/insertion reactions with a synthetic $Mg_{0.7}Mn_{6.1}O_{12}{\cdot}4.3H_2O$ todorokite. In this todorokite, Mg^{2+} locate at both (3×3) tunnel sites and octahedral Mn sites. Mg^{2+} in the tunnel sites can be extracted easily by an acid-treatment. The extraction reaction proceeds mostly by an ion-exchange reaction, but a small degree of redox reaction also occurs, because the manganese oxide contains some Mn^{III}. The metal ions can be inserted into the tunnel, and the insertion proceeds largely by an ion-exchange reaction. All alkali metal ions can enter the tunnel of the todorokite structure, but large ions, such as $(CH_3)_4N^+$ with an ionic radius of 3.5 Å, cannot.

Birnessite-type manganese oxide

Metal ions in the interlayer spaces of birnessite-type manganese oxides are easily extracted by an acid, and these metal ions are also exchanged easily with other cations. Since the birnessites show easy ion-exchange properties and can be used as precursors for the synthesis of tunnel manganese oxides, a large number of studies have been carried out by several authors.[91,110–116] The birnessite-type manganese oxides can be expressed by the general formula $(A_x)[\square_z Mn^{III}_y Mn^{IV}_{1-y-z}]O_2{\cdot}nH_2O$, where (), [], □, and A are interlayer sites, octahedral sites on the MnO_6 sheet, vacancies on the MnO_6 sheet, and metal ions in the interlayer sites, respectively, and x can be up to 0.7 for Na-birnessite. EXAFS studies[57,112,113] have indicated that there are two types of sites for metal ions locating in the interlayer. One is A site located on the crystal water sheet, and the other is B site located above and below the vacancies on the MnO_6 sheets, as shown in Fig. 14. The alkali and alkaline earth metal ions with large ionic radii are located at the A site, and transition metal ions

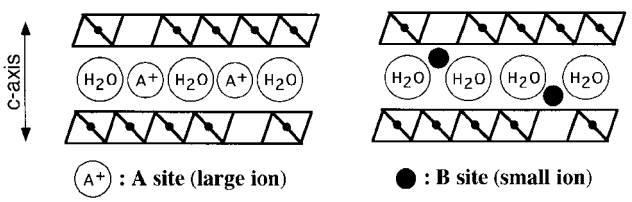

Fig. 14 Schematic representation of metal ion adsorptive sites in the interlayer of a birnessite structure: projection along *b*-axis.

with small ionic radii (*e.g.* Zn^{2+}, Cu^{2+}, Ni^{2+}, Co^{2+}, and Mn^{2+}) are located at the B site.

Recently, Drits *et al.*[114–116] have investigated the Na^+ extraction reaction by acid-treatment and ion-exchange reactions with metal ions for $Na_{0.3}Mn^{III}_{0.31}Mn^{IV}_{0.69}O_2$ birnessite. In the acidic solution, the disproportionation reaction of Mn^{III} occurs in the interlayer spaces, which causes formation of vacancies on the MnO_6 octahedral sheet. The dissolved Mn^{2+} can be re-adsorbed at the B site of birnessite. This is different from tunnel manganese oxides where the disproportionation reaction occurs on the surface of the crystal, and no vacancy occurs in the bulk crystal.

Since the layered structure of the birnessite is held mainly by an electrostatic attraction force between the negatively charged MnO_6 octahedral sheets and the positively charged metal ions in the interlayer, the charge density of MnO_6 octahedral sheet influences strongly the extraction/insertion reactions of cations. The extraction/insertion reactions cause a change in the basal spacing of the birnessite. When cations are inserted into interlayer spaces of the birnessite, the basal spacing of the birnessite with high charge density is more difficult to expand than that with low charge density. Specifically, it is difficult for large ions to enter the interlayer spaces of the birnessites with high charge density, and therefore such birnessite is suitable as an ion sieve. The birnessite with low charge density can be transformed to buserite by ion-exchanging with Mg^{2+} which has a strong hydration ability.[61,90,91] These birnessites are suitable as precursors for synthesis of large tunnel manganese oxides in the hydrothermal soft chemical process.

Other tunnel manganese oxides

Giovanoli *et al.*[117] have tried to extract Ba^{2+} from synthetic Ba-romanechite with acid. However, the romanechite structure changed to γ-MnO_2 after refluxing the Ba-romanechite in dilute nitric acid at 90–95 °C for 3 weeks. The authors concluded that the romanechite has no exchange properties. No studies on the extraction/insertion reactions of $Rb_{0.27}MnO_2$ and RUB-7 have been reported. The redox-type and ion-exchange-type reaction mechanisms described above would seem to be suitable also for these tunnel manganese oxides.

Besides the extraction reaction in the solution phase, several studies on the removal of template ions in melting salt and solid reactions have also been reported. The Na^+ template can be removed from $Na_{0.44}MnO_2$ by a Na^+/Li^+ exchange reaction in a $LiNO_3$/LiCl mixed melting salt at 260–275 °C.[19] NH_4^+ can be removed from NH_4-hollandite by solid reaction with LiOH at 300–400 °C.[66,67] Although these methods are developed for synthesis of lithium manganese oxides for lithium batteries, they can also be applied to manganese oxide ion-sieves, because Li^+ with its small ionic radius is more easily extracted from the tunnels than is the direct extraction of the template ions.

Ion-sieve and molecular-sieve properties

Ion-sieve properties

The template-extracted tunnel and layered manganese oxides show excellent ion-sieve properties for the adsorption of cations. Ooi *et al.*[102] have classified the adsorptive sites of manganese oxides into nonspecific and specific types. The adsorptive sites on the crystal surface are nonspecific ion-exchange sites, and the sites in the bulk of the crystal are specific sites which include specific ion-exchange and specific redox sites. The ion-exchange sites show higher acidity and stability than the redox sites. The adsorption of cations on specific sites show ion-sieve properties.

The ion-sieve properties of the manganese oxides have been characterized by pH titration and distribution coefficient measurement studies. The results of pH titration studies for spinel-, hollandite-, birnessite-, and todorokite-type ion-sieves are summarized in Fig. 15.[5] The spinel-type ion-sieves[38,102,118] show a remarkably larger adsorptive capacity for Li^+ than that for Na^+ and K^+, indicating that Li^+ with its small ionic radius can enter the tunnel of the spinel structure, where Na^+ and K^+ cannot. Na^+ and K^+ are adsorbed on the surface of the crystal, *i.e.*, non-specific adsorption. Li^+ are adsorbed on the specific sites after dehydration. Although divalent ions, such as Mg^{2+}, Ni^{2+}, and Co^{2+}, also have small ionic radii, they cannot enter the tunnel of a spinel structure, due to their dehydration energy being too large.[119]

The hollandite-type ion-sieves[11,63,108] show a large adsorptive capacity for K^+ at low pH range, due to a strong affinity toward K^+. At high pH range, the adsorptive capacity increases with a decrease of ionic radius, because the steric interaction between the metal ions in the tunnel become predominant. The large $(CH_3)_4N^+$ with an ionic radius of 3.5 Å cannot enter the (2×2) tunnel.

Birnessite-type ion-sieve shows a different adsorption behavior for small ions and large ions.[77,110] It shows a tribasic[77] or dibasic[110] acid behavior toward Li^+, and monobasic acid behavior toward Na^+, K^+, and Cs^+, because Li^+, with a small ionic radius, can be adsorbed on both the A and B sites of birnessite structure, but other large ions can only be adsorbed on the A sites.[77]

Similar behavior is also observed for the todorokite-type ion-sieve; dibasic acid behavior toward the small ions Li^+, Na^+, and K^+, and monobasic acid behavior to the large ion Cs^+.[59] The large ions are adsorbed on the center of the tunnel, but the small ions may be located close to the wall of the large tunnel. The small adsorptive capacity for $(CH_3)_4N^+$ indicates that it is too large to enter the tunnel of a todorokite-type ion-sieve. Since the tunnels of pyrolusite and ramsdellite are too small for metal ions to enter, metal ions can be adsorbed only on the surface sites.

The selectivities of manganese oxide ion-sieves for the adsorption of metal ions are strongly dependent on their structures.[5] Fig. 16 shows plots of the equilibrium distribution coefficient (K_d) against the effective ionic radius of the alkali metal ion for the manganese oxide ion-sieves. The selectivity sequences are $Na^+ < K^+ < Rb^+ < Cs^+ \ll Li^+$ for a spinel-type ion-sieve,[77,119] $Li^+ < Cs^+$, $Na^+ \ll Rb^+ < K^+$ for a hollandite-type ion-sieve,[11,63,108] $Li^+ < Na^+ < Cs^+$, $K^+ < Rb^+$ for a birnessite-type ion-sieve,[77] and $Li^+ < Na^+ < K^+ < Rb^+ < Cs^+$ for a todorokite-type ion-sieve.[59] A characteristic feature is that the selectivity sequences relate to the pore size of the ion-sieves. The spinel-type ion-sieve has extremely high selectivity for Li^+, the hollandite-type ion-sieve for K^+ and Rb^+, and birnessite-type ion-sieve with basal spacing of 0.72 nm for Rb^+. These features are explained on the basis of the ion-sieve effect of the manganese oxide lattices. The (1×3) tunnel is suitable in size for fixing Li^+, the (2×2) tunnel for fixing K^+ and Rb^+, and the interlayer space of birnessite for fixing Rb^+. The selectivity sequence for the todorokite-type ion-sieve is in agreement with the increasing order of the effective ionic radii of alkali metal ions. Namely, alkali metal ions can enter the (3×3) tunnel sites in the todorokite structure without steric effect, owing to the large tunnel size.

Feng *et al.*[5,77,108] have defined the highest K_d values around 0.07, 0.14, and 0.15 nm for the spinel-, hollandite-, and birnessite-type ion-sieves, respectively, as effective pore radii for these ion-sieves. The effective pore radius of the todorokite-type ion-sieve has been estimated as about 0.27 nm from the parameters of the todorokite structure by comparing it with the effective pore radius and the structural parameters of the hollandite-type ion-sieve.[59]

Molecular-sieve properties

The manganese oxides with large tunnel structure show molecular-sieve properties. Shen *et al.*[6] have studied the mol-

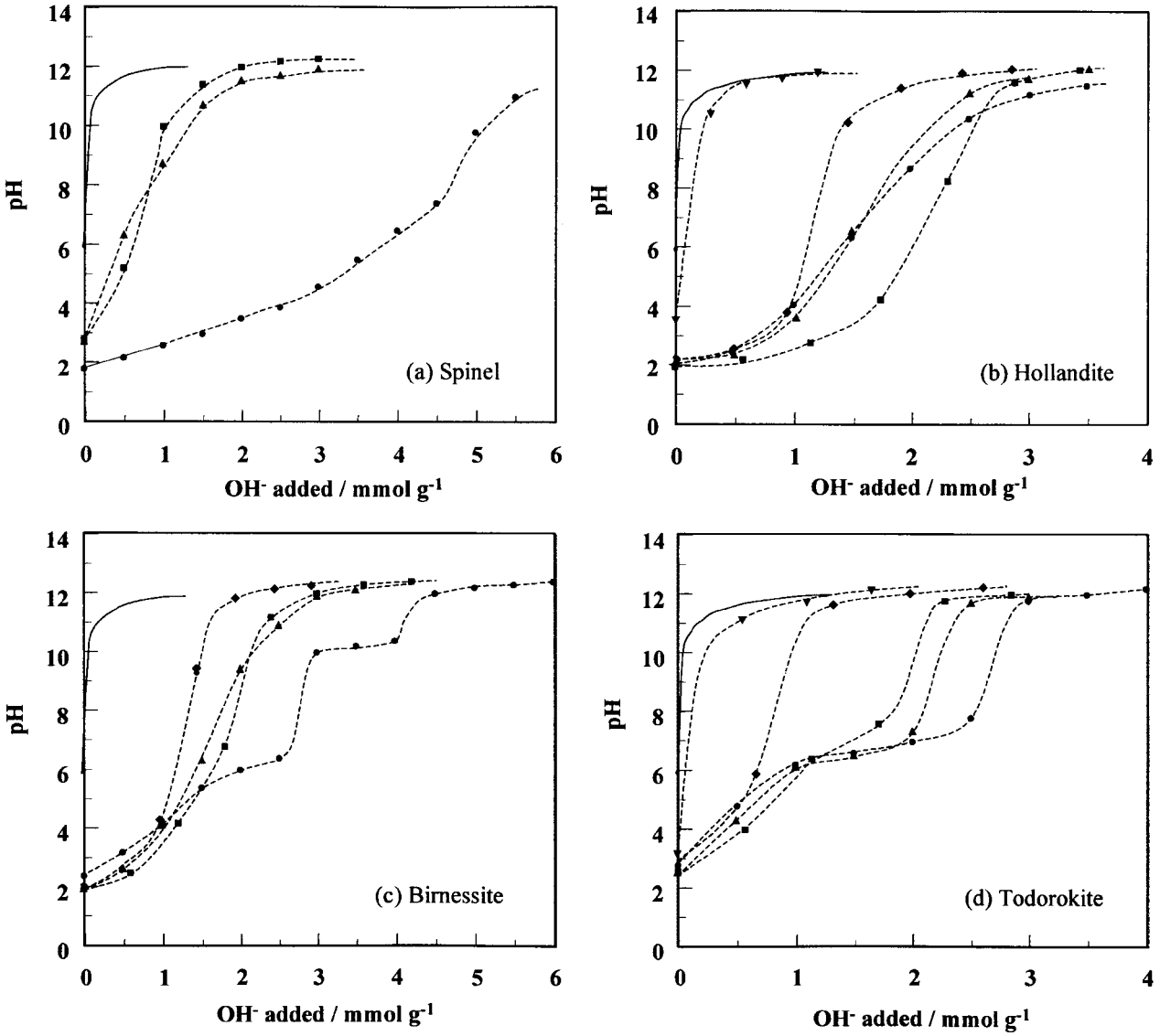

Fig. 15 pH titration curves of various kinds of manganese oxide ion-sieves. (a): spinel; (b): hollandite; (c): birnessite; (d): todorokite. Solid lines describe blank titration. ●: Li^+, ▲: Na^+, ■: K^+, ◆: Cs^+, ▼: $(CH_3)_4N^+$.

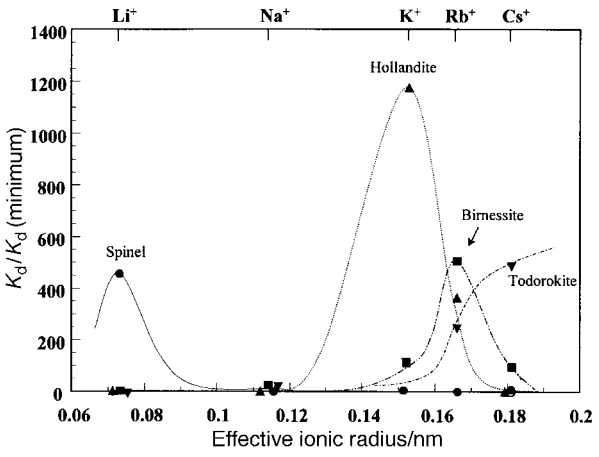

Fig. 16 Distribution coefficients (K_d) of alkali metal ions on the manganese oxide ion-sieves at pH 2 as a function of the effective ionic radius of alkali metal ions. ●: spinel, ▲: hollandite, ■: birnessite, ▼: todorokite.

ecular-sieve properties of Mg-todorokite. The todorokite shows significantly larger adsorptive capacities for C_6H_{12} and CCl_4 with size dimensions of 0.61 and 0.69 nm, respectively, than that for hexachloropentadiene and 1,3,5-triethylbenzene with size dimensions of 0.77 and 0.84 nm, respectively. The authors concluded that the todorokite-type molecular-sieve has a pore size of 0.69 nm. This barely differs from the effective pore size (0.54 nm) evaluated by the cation adsorptive studies.

The molecular-sieve properties of mesoporous manganese oxides have been investigated by Tian *et al.*[45] The organic surfactant templates can be removed from the tunnel of the hexagonal phase by calcining in air, and the molecular sieve is stable up to 1000 °C. N_2 sorption study shows that the template-removed hexagonal mesoporous molecular sieve has a uniform pore size of about 3.0 nm and a wall thickness of about 0.17 nm.

Electrochemical extraction/insertion reactions

Spinel-type manganese oxide

Li^+ can be extracted/inserted from/into the redox-type spinel $LiMn_2O_4$ by a topotactic electrochemical reaction in the aqueous phase. Reaction (2) can be divided into two half-cell

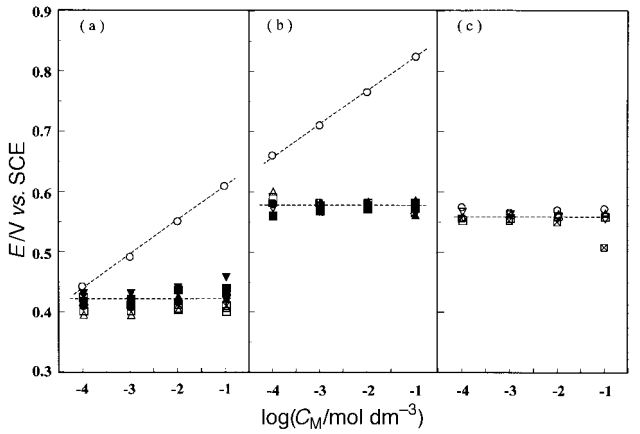

Fig. 17 Equilibrium potentials of the electrodes in solutions of alkali and alkaline earth metal chlorides. Electrode: a) $Pt/LiMn_2O_4$, b) Pt/λ-MnO_2, and c) Pt/Mn_2O_3. Electrolyte: LiCl (○), NaCl (△), KCl (□), RbCl (▽), CsCl (□), $MgCl_2$ (▲), $CaCl_2$ (■), $SrCl_2$ (▼), and $BaCl_2$ (◆). Reproduced by permission of The Electrochemical Society, Inc. from reference 10.

reactions;

$$(\ )[Mn^{IV}{}_2]O_4 + Li^+ + e^- \rightleftarrows (Li)[Mn^{III}Mn^{IV}]O_4 \quad (7)$$

$$OH^- \rightleftarrows 0.5H_2O + 0.25O_2 + e^- \quad (8)$$

Reaction (7) has been well analyzed on the basis of a one-phase solid solution model.[120–123] The electrode potential of the spinel-type manganese oxide electrode prepared on an inert metal conductor (*e.g.* Pt) can be described as;[10,100,124,125]

$$E = (\mu_e{}^m + \mu_{Li}{}^{1,0})/F + (RT/F)[\ln a_{Li} + (\partial \ln Z/\partial N_e) + (\partial \ln Z/\partial N_{Li})] \quad (9)$$

where $\mu_e{}^m$ is the chemical potential of the electron in the metal, $\mu_{Li}{}^{1,0}$ the standard chemical potential of Li^+ in the liquid phase, a_{Li} the activity of Li^+ in the liquid phase, N_i the number of species i in the solid phase, and Z the partition function associated with the distributions of electrons and Li^+ in the solid phase. When the Li/Mn ratio in the solid phase is constant, its electrode potential can be described as;

$$E = \text{Const.} + (RT/F)\ln a_{Li} \quad (10)$$

This shows that the electrode potential gives a Nernstian response to the activity of Li^+ in the liquid phase.

Equilibrium potentials of thin film electrodes of spinel-type manganese oxide ($Pt/Li_xMn_2O_4$, $0<x<1$) are shown in Fig. 17.[10] The potentials of $Pt/LiMn_2O_4$ and Pt/λ-MnO_2 electrodes relate to the logarithm of the concentration of Li^+ with near-Nernstian slopes [Fig. 17(a) and (b)]. However, the potentials of both electrodes are almost constant in a solution of other alkali metal ions or any alkaline earth metal ions regardless of metal ion concentration. These results indicate that the spinel-type manganese oxides respond only to Li^+; they correlate well with the results in which the redox-type insertion/extraction takes place only for Li^+ and not for other alkali metal ions, as described above. Thus, the λ-MnO_2 electrode is excellent as an Li^+-selective electrode. The Pt/Mn_2O_3 electrode does not respond to any alkali metal ions [Fig. 17(c)]. This suggests that the responses of the spinel electrodes to Li^+ can be ascribed to the porous structure of the spinel.

If the applied potential is swept, Li^+ insertion and extraction occur, which change the Li/Mn ratio in the solid phase. Cyclic voltammetry shows two peaks on both the cathodic and anodic sides according to the following two reactions (Fig. 18);[126]

$$0.5Li^+ + 2\lambda\text{-}MnO_2 + 0.5e^- \rightleftarrows Li_{0.5}Mn_2O_4$$

$$E \approx 0.85 \text{ V } \textit{vs.} \text{ SCE} \quad (11)$$

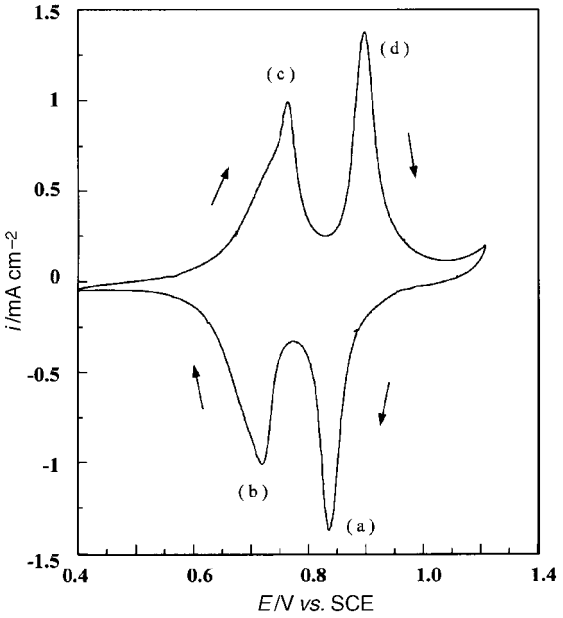

Fig. 18 Cyclic voltammogram of the Pt/λ-MnO_2 electrode in 1 mol dm^{-3} LiCl + 50 mmol dm^{-3} borate buffer solution (pH 7.5). Scan rate: 1 mV s^{-1}. Peaks (a) and (d) correspond to the insertion and extraction reactions (11), respectively. Peaks (b) and (c) correspond to the insertion and extraction reactions (12), respectively. Reproduced by permission of The Electrochemical Society, Inc. from reference 126.

$$0.5Li^+ + Li_{0.5}Mn_2O_4 + 0.5e^- \rightleftarrows LiMn_2O_4$$

$$E \approx 0.75 \text{ V } \textit{vs.} \text{ SCE} \quad (12)$$

The Li^+ insertion into the Pt/λ-MnO_2 electrode consists of three processes: (i) solution mass transport, (ii) dehydration and transfer at the solid surface, and (iii) solid-state diffusion. The diffusion and transfer coefficients and standard rate constants for reactions (11) and (12) have been evaluated by potential step chronoamperometry, cyclic voltammetry, and ac impedance spectroscopy.[126,127] The analyses have been carried out under the assumption that the solid-state diffusion of Li^+ is a rate-determining process. The results have shown that the chemical diffusion coefficient is in the range 1×10^{-12}–1×10^{-10} cm^2 s^{-1} and Li^+ diffuses by a hopping mechanism in the spinel phase.

In situ spectroscopic study of the Li^+ insertion has been performed by visible adsorption and Raman spectroscopy. Absorbance of the $Li_xMn_2O_4$ electrode prepared on a transparent conducting glass substrate changes with the Li^+ insertion.[128] This is attributed to the difference of absorption spectra between Mn^{III} and Mn^{IV}. The Raman spectra for λ-MnO_2 and $LiMn_2O_4$ show an intensity maximum at 593 and 628 cm^{-1} (I_{593} and I_{628}), respectively.[129] The parameter $\log(I_{593}/I_{628})$ correlates well with the electrochemical response for the Li^+ extraction/insertion. Both methods are applicable to the *in situ* monitoring of the electrochemical reaction.

Other manganese oxides

Electrochemical extraction/insertion reactions of metal ions with other types of manganese oxides have been studied. Todorokite-type and hollandite-type manganese oxides are characterized by cyclic voltammetry.[130] It has been concluded that the former is electroactive but the latter is not, because of the existence of the octahedral Mn^{2+} ions.

A thin layer electrode of birnessite-type manganese oxide was prepared and the extraction/insertion reactions of alkali metal ions with the electrode examined.[131] The chemical composition of the original electrode was K_xMnO_y ($x=0.33$ and $y\approx2$)with a basal spacing of $C_0=0.697$ nm. The anodic

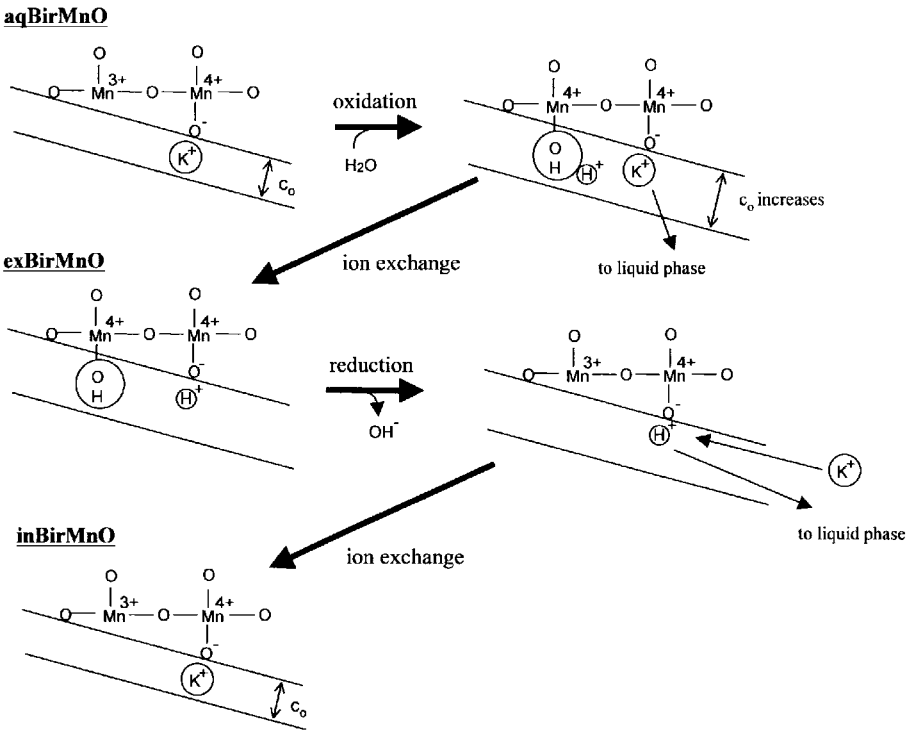

Fig. 19 Schematic diagrams of electrochemical extraction/insertion reactions of K^+ with birnessite-type manganese oxide. aqBirMnO: electrode after equilibration of the original electrode (orgBirMnO) in a KCl solution. exBirMnO: partly K^+-extracted electrode from the Pt/orgBirMnO or Pt/aqBirMnO electrodes by anodic sweep. Pt/inBirMnO: K^+-inserted electrode into the Pt/deBirMnO by cathodic sweep. Reprinted with permission from reference 131. Copyright 1997 American Chemical Society.

potential sweep on the electrode in an aqueous phase caused the extraction of K^+ with an increase in C_0. Quasi-reversible insertion of K^+ occurred with a subsequent cathodic sweep in a KCl solution. The electrochemical measurements suggested that K^+ is not electrochemically active in the extraction/insertion reactions but that H^+ is. The reaction, the scheme of which is shown in Fig. 19, proceeds based on the mechanism consisting of an electrochemical reaction (the redox reaction between Mn^{III} and Mn^{IV}) and an ion-exchange reaction between K^+ and H^+.

Applications as adsorbents and catalysts

Advanced separation and sensing technology has been developed by application of the ion-sieve properties of the manganese oxides. The spinel-type ion-sieves show excellent selective adsorptive properties for lithium from seawater and dilute solutions.[51,96,97,119,132] The ion-exchange-type spinel $H_{1.33}Mn_{1.67}O_4$ has the largest lithium uptake (18 mg g^{-1}) from seawater at a lithium concentration of 0.17 ppm.[8] A study on repeated adsorption and desorption of an ion-sieve granulated with polyvinyl chloride as a binder indicated that it is a chemically stable and promising adsorbent for lithium recovery from seawater.[8] Electrochemical recovery of lithium from aqueous solutions has been examined by using the redox-type spinel ion-sieve electrode (Pt/λ-MnO_2).[133] The lithium uptake is 11 mg g^{-1} from geothermal water with a lithium concentration of 0.75 mM. The ion-sieve electrode can also be applied to sensing Li^+ in aqueous solutions.[10,134] The hollandite-type ion-sieve shows high selectivities for K^+ and Rb^+, and can be applied to the separation of K^+ and Rb^+ from their dilute solutions.[11,51,52,63]

Several studies on the catalytic properties of porous manganese oxide crystals have been carried out. Cao *et al.*[7] have shown that manganese oxides can be used as photocatalysts for the oxidation of propan-2-ol to acetone. High activities correlate with the higher oxidation state of manganese oxides, large surface oxygen concentrations, and the presence of hydroxy groups on the surfaces of amorphous, pyrolusite, hollandite, and todorokite manganese oxides. A study on the catalytic property of mesoporous manganese oxides shows that catalytic oxidation of cyclohexane and *n*-hexane in aqueous solutions in a batch reactor show conversions of *ca.* 10 and 8%, respectively.[45]

Conclusions

The tunnel and layered manganese oxides constitute a large family of porous materials with pore size from ultramicropores to mesopores. The structural frameworks of the manganese oxide porous crystals consist mainly of MnO_6 octahedral units shared by corners or edges. For the preparation of manganese oxide porous crystals, metal ions and organic ions can be used as templates to control their pore dimensions in various synthesis processes. The hydrothermal soft chemical process is a potentially useful method of using a template to design the porous structures.

The metal ion templates in the porous manganese oxides can be removed by chemical and electrochemical topotactic reactions. Cations can be reinserted topotactically into the template-free manganese oxides. There are two types of sites (redox- and ion-exchange-type) in the insertion/extraction reactions. The presence of Mn^{III} relates to formation of the redox-type sites, and the presence of Mn defects to the ion-exchange sites.

The manganese oxides show ion sieve properties in insertion reactions. The spinel-, hollandite-, birnessite-, and todorokite-type ion-sieves have effective pore radii of 0.07, 0.14, 0.15, and 0.27 nm, respectively. The ion-exchange type manganese oxides can be applied to the development of advanced preparation technology, and the redox-type to the development of sensing technology. The porous manganese oxides also show molecular sieve properties. Primary studies show that the manganese oxides are promising catalytic materials, and have

high activities for oxidation reactions. Elucidation of the relation between the crystal structure and catalytic activity is an important subject for the application of manganese oxides in this field.

Other porous transition metal oxides can also be used as ion sieves and molecular-sieves similar to the manganese oxides described here. Although several studies on mesoporous transition metal oxides and their molecular-sieve properties have been reported, there are only a few studies on microporous materials and ion-sieve properties. The preparation of a new type of microporous transition metal oxide is significant for the development of their ion-sieves.

References

1 S. L. Suib, *Chem. Rev*., 1993, **93**, 803.
2 Q. Huo, D. I. Margolese, U. Ciesla, P. Feng, T. E. Gier, P. Sieger, R. Leon, P. M. Petroff, F. Schuth and G. D. Stucky, *Nature*, 1994, **368**, 317.
3 D. M. Antonelli, A. Nakahira and J. Y. Ying, *Inorg. Chem.*, 1996, **35**, 3126.
4 R. G. Burns and V. M. Burns, *Manganese Dioxide Symposium*, Tokyo, 1980, vol. 2, p. 97.
5 Q. Feng, H. Kanoh, Y. Miyai and K. Ooi, *1995 Int. Conf. Ion Exchange*, *Proceedings*, 1995, p. 141.
6 Y. F. Shen, R. P. Zerger, R. N. DeGuzman, S. L. Suib, L. McCurdy, D. I. Potter and C. L. O'Young, *Science*, 1993, **260**, 511.
7 H. Cao and S. L. Suib, *J. Am. Chem. Soc.*, 1994, **116**, 5334.
8 K. Ooi, Q. Feng, H. Kanoh and Y. Miyai, *1995 Int. Conf. Ion Exchange*, *Proceedings*, 1995, p. 365.
9 K. Ooi, Q. Feng, H. Kanoh, T. Hirotsu and T. Oi, *Separation Sci. Technol.*, 1995, **30**, 3761.
10 H. Kanoh, Q. Feng, Y. Miyai and K. Ooi, *J. Electrochem. Soc.*, 1993, **140**, 3162.
11 M. Tsuji and M. Abe, *Bull. Chem. Soc. Jpn.*, 1985, **58**, 1109.
12 R. Koksbang, J. Barker, H. Shi and M. Y. Saidi, *Solid State Ionics*, 1996, **84**, 1.
13 M. M. Thackeray, *Symp. Rechargeable Lithium and Lithium-Ion Batteries 1994*, *Proceedings*, 1995, p. 233.
14 Q. Feng, H. Kanoh, K. Ooi, M. Tani and Y. Nakacho, *J. Electrochem. Soc.*, 1994, **141**, L135.
15 C. S. Johnson, D. W. Dees, M. F. Mansuetto, M. M. Thackeray, D. R. Vissers, D. Argyriou, C.-K. Loong and L. Christensen, *J. Power Sources*, 1997, **68**, 570.
16 P. Strobel and C. Mouget, *Mater. Res. Bull.*, 1993, **28**, 93.
17 P. Le Goff, N. Baffier, S. Bach and J. P. Pereira-Ramos, *Mater. Res. Bull.*, 1996, **31**, 63.
18 A. R. Armstrong and P. G. Bruce, *Nature*, 1996, **381**, 499.
19 A. R. Armstrong, H. Huang, R. A. Jennings and P. G. Bruce, *J. Mater. Chem.*, 1998, **8**, 255.
20 Y. Moritomo, A. Asamitsu, H. Kuwahara and Y. Tokura, *Nature*, 1996, **380**, 141.
21 Y. Shimakawa, Y. Kubo and T. Manako, *Nature*, 1996, **379**, 53.
22 S. Mori, C. H. Chen and S.-W. Cheong, *Nature*, 1998, **392**, 473.
23 R. V. Helmolt, J. Wecker, B. Holzapfel, L. Schultz and K. Samwer, *Phys. Rev. Lett.*, 1993, **71**, 2332.
24 M. McCormack, S. Jin, T. H. Fleming, J. M. Phillips and R. Ramesh, *Appl. Phys. Lett*., 1994, **64**, 3045.
25 C. N. R. Rao, A. K. Cheetham and R. Mahesh, *Chem. Mater.*, 1997, **8**, 2421.
26 S. Turner and P. R. Buseck, *Science*, 1981, **212**, 1024.
27 R. Giovanoli, *Chem. Erde*, 1985, **44**, 227.
28 R. M. Potter and G. R. Rossman, *Am. Mineral*., 1979, **64**, 1199.
29 A. D. Wadsley, *Acta Crystallogr*., 1953, **6**, 433.
30 O. Tamada and N. Yamamoto, *Mineral. J.*, 1986, **13**, 130.
31 P. Strouff and J. Boulegue, *Am. Mineral.*, 1988, **73**, 1162.
32 P. Strobel, J.-C. Charenton and M. Lenglet, *Rev. Chim. Miner.*, 1987, **24**, 199.
33 S. Turner and P. R. Buseck, *Nature*, 1983, **304**, 143.
34 M. Voinov, *Electrochim. Acta*., 1982, **27**, 833.
35 S. Turner and P. R. Buseck, *Science*, 1979, **203**, 456.
36 W. I. F. David, M. M. Thackeray, P. G. Bruce and J. B. Goodenough, *Mater. Res. Bull.*, 1984, **19**, 99.
37 G. Blasse, *Philips Res. Rep.*, 1964, Suppl. No. 3.
38 Q. Feng, Y. Miyai, H. Kanoh and K. Ooi, *Langmuir*, 1992, **8**, 1861.
39 M. M. Thackeray, A. de Kock, M. H. Rossouw, D. Liles, R. Bittihn and D. Hoge, *J. Electrochem. Soc.*, 1992, **139**, 363.
40 J.-P. Parant, R. Olazcuaga, M. Devalette, C. Fouassier and P. Hagenmuller, *J. Solid State Chem.*, 1971, **3**, 1.
41 J. N. Reimers, E. W. Fuller, E. Rossen and J. R. Dahn, *J. Electrochem. Soc., 1993,* **140**, 3396.
42 M. H. Rossouw, D. C. Liles and M. M. Thackeray, *J. Solid State Chem.*, 1993, **104**, 464.
43 T. Rziha, H. Gies and J. Rius, *Eur. J. Mineral.*, 1996, **8**, 675.
44 Ph. Boullay, M. Hervieu and B. Raveau, *J. Solid State Chem.*, 1997, **132**, 239.
45 Z.-R. Tian, W. Tong, J.-Y. Wang, N.-G. Duan, V. V. Krishnan and S. L. Suib, *Science*, 1997, **276**, 926.
46 Q. Huo, D. I. Margolese, U. Ciesla, D. G. Demuth, P. Feng, T. E. Gier, P. Sieger, A. Firouzi, B. F. Chmelka, F. Schuth and G. D. Stucky, *Chem. Mater.*, 1994, **6**, 1176.
47 A. Bergstein, J. Sestak, P. Holba, P. Kleinert and A. Funke, *Czech. J. Phys.*, 1967, **B17**, 686.
48 C. Masquelier, M. Tabuchi, K. Ado, R. Kanno, Y. Kobayashi, Y. Maki, O. Nakamura and J. B. Goodenough, *J. Solid State Chem.*, 1996, **123**, 255.
49 B. Ammundsen, D. J. Jones, J. Roziere and G. R. Burns, *Chem. Mater.*, 1995, **7**, 2151.
50 B. Ammundsen, D. J. Jones, J. Roziere and G. R. Burns, *Chem. Mater*., 1996, **8**, 2799.
51 K. Ooi, Y. Miyai and S. Katoh, *Sep. Sci. Technol.*, 1987, **22**, 1779.
52 Y. Tanaka and M. Tsuji, *Mater. Res. Bull.*, 1994, **29**, 1183.
53 W. Tang, H. Kanoh and K. Ooi, *J. Solid State Chem.*, in press.
54 R. Giovanoli, E. Stahli and W. Feitknecht, *Helv. Chim. Acta*, 1970, **53**, 209.
55 R. Giovanoli, E. Stahli and W. Feitknecht, *Helv. Chim. Acta*, 1970, **53**, 453.
56 J. Luo and S. L. Suib, *J. Phys. Chem. B*, 1997, **101**, 10403.
57 P. Strobel, J. Durr, M.-H. Tullire and J.-C. Charenton, *J. Mater. Chem.*, 1993, **3**, 453.
58 T. Ohzuku, H. Fukuda and T. Hirai, *Chem. Express*., 1987, 543.
59 Q. Feng, H. Kanoh, Y. Miyai and K. Ooi, *Chem. Mater.*, 1995, **7**, 1722.
60 Q. Feng, E.-H. Sun, K. Yanagisawa and N. Yamasaki, *J. Ceramic Soc. Jpn.*, 1997, **105**, 564.
61 Q. Feng, K. Yanagisawa and N. Yamasaki, *J. Ceram. Soc. Jpn.*, 1996, **104**, 897.
62 Q. Feng, K. Yanagisawa and N. Yamasaki, *J. Mater Sci. Lett.*, 1997, **16**, 110.
63 M. Tsuji and M. Abe, *Solvent Extr. Ion Exch.*, 1984, **2**, 253.
64 J. B. Fernandes, B. D. Desai and V. N. Kamat Dalal, *Electrochim. Acta*, 1984, **29**, 181.
65 R. N. DeGuzman, Y.-F. Shen, E. J. Neth, S. L. Suib, C.-L. O'Young, S. Levine and J. M. Newsam, *Chem. Mater.*, 1994, **6**, 815.
66 Ph. Botkovitz, Ph. Deniard, M. Tournoux and R. Brec, *J. Power Sources*, 1993, **43–44**, 657.
67 M. A. Humber, Ph. Biensan, M. Broussely, A. Lecerf, A. Dolle and H. Ladhily, *J. Power Sources*, 1993, **43–44**, 681.
68 T. Nishimura and Y. Umetsu, *J. Mining Mater. Proc. Inst. Jpn.*, 1992, **108**, 373.
69 J. Luo and S. L. Suib, *Chem. Commun.*, 1997, 1031.
70 P. Barboux, J. M. Tarascon and F. K. Shokoohi, *J. Solid State Chem.*, 1991, **94**, 185.
71 T. Takada, H. Hayakawa and E. Akiba, *J. Solid State Chem.*, 1995, **115**, 420.
72 T. Takada, H. Hayakawa, T. Kumagai and E. Akiba, *J. Solid State Chem.*, 1996, **121**, 79.
73 S. Bach, M. Henry, N. Baffier and J. Livage, *J. Solid State Chem.*, 1990, **88**, 325.
74 S. Bach. J. P. Pereira-Ramos, N. Baffier and R. Messina, *Electrochim. Acta*, 1991, **36**, 1595.
75 S. Ching, D. J. Petrovay, M. L. Jorgensen and S. L. Suib, *Inorg. Chem.*, 1997, **36**, 883.
76 S. Ching, J. L. Roark, N. Duan and S. L. Suib, *Chem. Mater.*, 1997, **9**, 750.
77 Q. Feng, H. Kanoh, Y. Miyai and K. Ooi, *Chem. Mater.*, 1995, **7**, 1226.
78 Q. Feng, N. Yamasaki, K. Yanagisawa and K. Ooi, *J. Mater. Sci. Lett.*, 1996, **15**, 963.
79 S. Hirano, R. Narita and S. Naka, *Mater. Res. Bull.*, 1984, **19**, 1229.
80 J. Morales, J. J. Navas and J. L. Tirado, *Solid State Ionics*, 1990, **44**, 125.
81 T. Endo, S. Kume, M. Shimada and M. Koizumi, *Miner. Mag.*, 1974, **39**, 559.
82 T. Ohzuku, M. Kitagawa, K. Sawai and T. Hirai, *J. Electrochem. Soc.*, 1991, **138**, 360.

83 C. S. Johnson, D. W. Dees, M. F. Mansuetto, M. M. Thackeray, D. R. Vissers, D. Argyriou, C.-K. Loong and L. Christensen, *J. Power Sources*, 1997, **68**, 570.
84 M. H. Rossouw, D. C. Liles, M. M. Thackeray, W. I. F. David and S. Hull, *Mater. Res. Bull.*, 1992, **27**, 221.
85 N. Yamamoto and O. Tamada, *J. Cryst. Growth*, 1985, **73**, 199.
86 N. Yamamoto and O. Tamada, *Bull. Inst. Chem. Res.*, *Kyoto Univ.*, 1986, **64**, 218.
87 Q. Feng, K. Yanagisawa and N. Yamasaki, *Chem. Commun.*, 1996, 1607.
88 A. D. Wadsley, *Am. Mineral.*, 1950, **35**, 485.
89 D. C. Golden, C. C. Chen and J. B. Dixon, *Science*, 1986, **231**, 717.
90 D. C. Golden, C. C. Chen and J. B. Dixon, *Clays Clay Miner.*, 1987, **35**, 271.
91 Q. Feng, K. Yanagisawa and N. Yamasaki, *J. Porous Mater.*, 1998, **5**, 153.
92 Q. Feng, C. Honbu, K. Yanagisawa and N. Yamasaki, *Chem. Lett.*, 1998, 757.
93 C.-C. Chen, D. C. Golden and J. B. Dixon, *Clays Clay Miner.*, 1986, **34**, 565.
94 R. Giovanoli and B. Balmer, *Chimia*, 1981, **35**, 53.
95 S.-T. Wong and S. Cheng, *Inorg. Chem.*, 1992, **31**, 1165.
96 V. V. Vol'klin, G. V. Leont'eva and S. A. Onorin, *Neorg. Mater.*, 1973, **9**, 1041.
97 G. V. Leont'eva and V. V. Vol'klin, *Zh. Prikl. Khim.*, 1971, **44**, 2615.
98 J. C. Hunter, *J. Solid State Chem.*, 1981, **39**, 142.
99 K. Ooi, Y. Miyai, S. Katoh, H. Maeda and M. Abe, *Chem. Lett*., 1988, 989.
100 K. Ooi, Y. Miyai, S. Katoh, H. Maeda and M. Abe, *Langmuir*, 1989, **5**, 150.
101 X. M. Shen and A. Clearfield, *J. Solid State Chem.*, 1986, **64**, 270.
102 K. Ooi, Y. Miyai and J. Sakakihara, *Langmuir*, 1991, **7**, 1167.
103 K. Sato, D. M. Poojary, A. Clearfield, M. Kohno and Y. Inoue, *J. Solid State Chem.*, 1997, **131**, 84.
104 Q. Feng, Y. Miyai, H. Kanoh and K. Ooi, *Chem. Mater.*, 1993, **5**, 311.
105 Q. Feng, H. Kanoh Y. Miyai and K. Ooi, *Chem. Mater.*, 1995, **7**, 379.
106 Y.-F. Liu, Q. Feng and K. Ooi, *J. Colloid Interface Sci.*, 1994, **163**, 130.
107 M. Tsuji and S. Komarneni, *J. Mater. Res.*, 1993, **8**, 611.
108 Q. Feng H. Kanoh, Y. Miyai and K. Ooi, *Chem Mater.*, 1995, **7**, 148.
109 C. Frondel, U. B. Marvin and J. Ito, *Am. Mineral.*, 1960, **45**, 871.
110 M. Tsuji, S. Komarneni, Y. Tamaura and M. Abe, *Mater. Res. Bull.*, 1992, **27**, 741.
111 P. Le, Goff, N. Baffier, S. Bach and J. P. Perira-Ramos, *Mater, Res. Bull.*, 1996, **31**, 63.
112 G. Arrhenius, K. Cheung, S. Crane, M. Fisk, J. Frazer, J. Korkisch, T. Mellin, S. Nakao, A. Tsai and G. Woef, *Colloques Intern Centre National de la Recherche Scientifique*, 1979, No. 289, p. 333.
113 S. Crane, Ph. D. Thesis, Scripps Inst. Oceanogr., La Jolla, CF, 1979.
114 V. A. Drits, E. Silvestre, A. I. Gorshkov and A. Manceau, *Am. Mineral*., 1997, **82**, 946.
115 E. Silvestre, A. Manceau and V. A. Drits, *Am. Mineral*., 1997, **82**, 962.
116 V. A. Drits, B. Lanson, A. I. Gorshkov and A. Manceau, *Am. Mineral.*, 1998, **83**, 97.
117 R. Giovanoli and B. Balmer, *Chimia*, 1983, **11**, 424.
118 K. Ooi, Y. Miyai, S. Katoh, H. Maeda and M. Abe, *Bull. Chem. Soc. Jpn.*, 1988, **61**, 407.
119 K. Ooi, Y. Miyai and S. Katoh, *Solvent Extr. Ion Exch.*, 1987, **5**, 561.
120 D. T. Ferrell and W. C. Vosburgh, *J. Electrochem. Soc.*, 1951, **98**, 334.
121 W. C. Maskell, J. A. E. Shaw and F. L. Tye, *Electrochim. Acta*, 1983, **28**, 225.
122 S. Atlung and T. Jacobsen, *Electrochim. Acta*, 1981, **26**, 1447.
123 T. Ohzuku, K. Sawai and T. Hirai, *J. Electrochem. Soc.*, 1985, **132**, 2828.
124 Y. Kanzaki, A. Taniguchi and M. Abe, *J. Electrochem. Soc*., 1991, **138**, 333.
125 W. Li, W. R. McKinnon and J. R. Dahn, *J. Electrochem. Soc.*, 1994, **141**, 2310.
126 H. Hanoh, Q. Feng, Y. Miyai and K. Ooi, *J. Electrochem. Soc.*, 1995, **142**, 702.
127 H. Kanoh, Q. Feng, T. Hirotsu and K. Ooi, *J. Electrochem. Soc.*, 1995, **142**, 2610.
128 H. Kanoh, T. Hirotsu and K. Ooi, *J. Electrochem. Soc.*, 1996, **143**, 905.
129 H. Kanoh, W. Tang and K. Ooi, *Electrochem. Solid State Lett.*, 1998, **1**, 17.
130 R. N. De Guzman, Y. Shen, B. R. Shaw, S. L. Suib and C. O'Young, *Chem. Mater.*, 1993, **5**, 1395.
131 H. Kanoh, W. Tang, Y. Makita and K. Ooi, *Langmuir*, 1997, **13**, 6845.
132 K. Ooi, Y. Miyai and S. Katoh, *Sep. Sci. Technol.*, 1986, **21**, 755.
133 H. Kanoh, K. Ooi, Y. Miyai and S. Katoh, *Sep. Sci. Technol.*, 1993, **28**, 643.
134 H. Kanoh, K. Ooi, Y. Miyai and S. Katoh, *Langmuir*, 1991, **7**, 1841.

Paper 8/05369C